Published in final edited form as:
*Neuroscience*. 2009 June 30; 161(2): 635–654. doi:10.1016/j.neuroscience.2009.03.056.

# Altered mnemonic functions and resistance to NMDA receptor antagonism by forebrain conditional knockout of glycine transporter 1

**Philipp Singer**[1], **Benjamin K. Yee**[1], **Joram Feldon**[1], **Takuji Iwasato**[2], **Shigeyoshi Itohara**[3], **Thomas Grampp**[4], **George Prenosil**[4], **Dietmar Benke**[4], **Hanns Möhler**[4,5], and **Detlev Boison**[6]

[1] *Laboratory of Behavioral Neurobiology, ETH Zurich, 8603 Schwerzenbach, Switzerland* [2] *Department of Developmental Genetics, National Institute of Genetics, 1111Yata, Mishima, Shizuoka 411-8540, Japan* [3] *Laboratory for Behavioral Genetics, RIKEN Brain Science Institute, Wako, Saitama 351-0198, Japan* [4] *Institute of Pharmacology and Toxicology, University of Zurich, 8057 Zurich, Switzerland* [5] *Institute of Pharmaceutical Sciences, ETH Zurich and Collegium Helveticum, 8093 Zurich, Switzerland* [6] *R. S. Dow Neurobiology Laboratories, Legacy Research, Portland, Oregon 97232, USA*

## Abstract

Converging evidence from pharmacological and molecular studies has led to the suggestion that inhibition of glycine transporter 1 (GlyT1) constitutes an effective means to boost *N*-methyl-D-aspartate receptor (NMDAR) activity by increasing the extra-cellular concentration of glycine in the vicinity of glutamatergic synapses. However, the precise extent and limitation of this approach to alter cognitive function, and therefore its potential as a treatment strategy against psychiatric conditions marked by cognitive impairments, remains to be fully examined. Here, we generated mutant mice lacking GlyT1 in the entire forebrain including neurons and glia. This conditional knockout system allows a more precise examination of GlyT1 down-regulation in the brain on behaviour and cognition. The mutation was highly effective in attenuating the motor-stimulating effect of acute NMDAR blockade by phencyclidine, although no appreciable elevation in NMDAR-mediated EPSC was observed in the hippocampus. Enhanced cognitive performance was observed in spatial working memory and object recognition memory while spatial reference memory and associative learning remained unaltered. These findings provide further credence for the potential cognitive enhancing effects of brain GlyT1 inhibition. At the same time, they indicated potential phenotypic differences when compared with other constitutive and conditional GlyT1 knockout lines, and highlighted the possibility of a functional divergence between the neuronal and glia subpopulations of GlyT1 in the regulation of learning and memory processes. The relevance of this distinction to the design of future GlyT1 blockers as therapeutic tools in the treatment of cognitive disorders remains to be further investigated.

Correspondence to D. Boison at address above: Phone: (503) 413 1754, Fax: (503) 413 5465, E-mail: E-mail: dboison@downeurobiology.org.

**Keywords**

GlyT1; NMDA receptor; latent inhibition; learning; psychopharmacology; schizophrenia

## INTRODUCTION

By binding to the glycine-B site, glycine acts as an obligatory co-agonist of glutamate at the *N*-methyl-D-aspartate receptor (NMDAR). Local glycine levels in the vicinity of glutamatergic synapses containing NMDARs are tightly regulated by the glycine transporter 1 (GlyT1), which mediates glycine re-uptake from the synaptic cleft into neurons and adjacent glia cells (Eulenburg et al., 2005; Betz et al., 2006). GlyT1 therefore constitutes an important up-stream modulator of NMDAR activity (Bergeron et al., 1998) and as such represents a potential target for interventions aimed to modulate NMDAR function. An increasing body of evidence indicates that pharmacological blockade or molecular disruption of GlyT1 potentiates glutamatergic transmission and exhibits activity in animal models of neuropsychiatric conditions (Kinney et al., 2003; Tsai et al., 2004; Aragon and Lopez-Corcuera, 2005; Gabernet et al., 2005; Martina et al., 2005; Lindsley et al., 2006; Yee et al., 2006; Singer et al., 2007; Sur and Kinney, 2007). Given that NMDARs assume important roles in cognitive processes underlying learning and memory (Tang et al., 1999), increased availability of glycine at glutamatergic synapses through inhibition of GlyT1 mediated re-uptake may provide novel therapeutic avenues to treat cognitive impairments in a number of psychiatric conditions and may even prove useful in boosting specific mental function in healthy subjects.

The therapeutic potential of inhibiting GlyT1 function has been supported by several studies of GlyT1 inhibitors demonstrating their pro-cognitive effects in preclinical models of cognitive deficits linked to schizophrenia (Depoortere et al., 2005; Lipina et al., 2005; Boulay et al., 2008; Hashimoto et al., 2008; Karasawa et al., 2008; Black et al., 2009). Enhanced mnemonic performance under non-pathological condition was recently demonstrated with the GlyT1 blocker SSR504734 on working memory (Singer et al., 2009a), and experience dependent selective attention (Black et al., 2009). With a genetic deletion approach, Tsai et al. (2004) also reported a tentative enhancing effect on water maze learning. More clear evidence for the presence of promnesic phenotypes have since been reported in mutant mice with forebrain neuron specific deletion of GlyT1 (Yee et al., 2006; Singer et al., 2007), which in many respects parallel the findings based on pharmacological GlyT1 blockade mentioned earlier.

To extend and build on the encouraging findings outlined above, we generated here knockout mice with forebrain GlyT1 deficiency affecting both neurons and glia cells, to allow the further assessment of the behavioural effects of reduced GlyT1 functionality and the concomitant effect on NMDAR functions. This includes cognitive assays that are sensitive to pharmacological and molecular manipulations targeted at the NMDAR or GlyT1, including spatial reference and working memory in the water maze, object recognition memory, and latent inhibition (LI) of associative learning. Working memory function is highly sensitive to a number of glutamatergic interventions within forebrain structures including hippocampus and prefrontal cortex (Verma and Moghaddam, 1996; Kawabe et al., 1998a; Kawabe et al., 1998b; Aura and Riekkinen, 1999; Steele and Morris, 1999; Lee and Kesner, 2002; Nakazawa et al., 2003; Yoshihara and Ichitani, 2004), and working memory performance can be enhanced by the GlyT1 inhibitor SSR504734 (Singer et al., 2008). Similarly, spatial reference memory is impaired by several molecular and pharmacological interventions designed to reduce NMDARs function within the hippocampus (McHugh et al., 1996; Tsien et al., 1996; Tonegawa et al., 2003). The possibility that GlyT1 deletion may enhance reference memory learning has been demonstrated previously by Tsai et al. (2004), although the reported pro-cognitive effect appears limited in size. Although object recognition memory appears to depend

on the integrity of rhinal cortices (Davachi and Goldman-Rakic, 2001; Bartko et al., 2007) rather than the hippocampus, it is also sensitive to NMDAR manipulations (Pitsikas et al., 2008), and performance can be enhanced by GlyT1 gene deletion (Singer et al., 2007), which parallels the outcome on social recognition memory by GlyT1 inhibitor (Depoortere et al., 2005).

NMDAR-mediated neurophysiology was evaluated by comparing the effects of the mutation on evoked NMDAR and AMPAR-mediated excitatory postsynaptic currents (eEPSCs). *In vivo* NMDAR functionality at the system level was evaluated by examining the animals' response to an acute systemic challenge of phencyclidine (PCP), an NMDA antagonist. The ability of GlyT1 inhibitor to attenuate the motor stimulant effect of NMDAR antagonist is a robust finding (Harsing et al., 2003; Depoortere et al., 2005; Boulay et al., 2008; Singer et al., 2009a). Surprisingly, constitutive heterozygous GlyT1 knockout did not alter the acute response to the NMDAR antagonist MK-801 (Tsai et al., 2004), yet conditional forebrain neuron GlyT1 knockout significantly reduced the motor stimulating effects of acute NMDAR antagonist treatment (Yee et al., 2006; Mohler et al., 2008). Finally, given recent evidence suggesting that systemic GlyT1 inhibiting drug (Singer et al., 2009a) as well as genetic deletion of GlyT1 (Yee et al., 2006) may modify dopaminergic neurotransmission (Javitt et al., 2000; Depoortere et al., 2005; Javitt et al., 2005), the response to an acute systemic dose of amphetamine, a dopamine releasing agent, was also examined here.

The present study represents another critical evaluation of the behavioral and physiological impacts of GlyT1 down-regulation in the brain by examining another novel mouse line with targeted deletion of GlyT1. This adds to previous attempts in the identification and characterization of the potential therapeutic potentials as well as limitations of GlyT1 blockade.

## EXPERIMNETAL PROCEDURES

### Generation of Emx1Cre:GlyT1tm1.2fl/fl mice

A strategy similar to the creation of the neuronal forebrain selective GlyT1 knockout mice *CamKIIαCre:GlyT1tm1.2fl/fl* (CamKII/GlyT1-KO) (Yee et al., 2006) was employed in the present study to create the neuron plus glia forebrain selective GlyT1 knockout mice *Emx1Cre:GlyT1tm1.2fl/fl* (EMX/GlyT1-KO) used for the experiments described here. Briefly, to achieve neuron plus glia forebrain-selective recombination of the floxed *GlyT1* allele, conditional GlyT1 knockout mice *GlyT1tm1.2fl/fl* (Yee et al., 2006) were bred with $Emx1^{Cre/Cre}$ mice, which contain a Cre-recombinase gene "knocked in" into the endogenous Emx1 locus (Iwasato et al., 2000) resulting in ubiquitous dorsal telencephalon specific expression of Cre in both neurons and astrocytes and minor ectopic expression of Cre beyond the forebrain. Further breeding resulted in *Emx1Cre:GlyT1tm1.2fl/fl* mice (referred to in the following as "mutant"). Subjects used in this study were generated by breeding *Emx1Cre:GlyT1tm1.2fl/fl* mice with *GlyT1tm1.2fl/fl* mice (referred to in the following as "control") thus producing mutants and controls in a 1:1 ratio as littermates and keeping mutants homozygous for the *GlyT1tm1.2fl* allele and heterozygous for the $Emx1^{Cre}$ allele. All subjects were generated and maintained on a pure C57BL/6 background. Genotyping was performed as described previously (Yee et al., 2006) using the following primers: o139: 5′-CCTAACCCATGGCCAGGACC-3′, GlyT1 specific antisense primer flanking the PGK-neomycin cassette; o184: 5′-CATCGCCTTCTATCGCCTTCTTGACG-3′, sense primer specific for the PGK-neomycin cassette; o228: 5′-GTCAACCTGACTCCTAGCCCTGTACC-3′, GlyT1 specific antisense primer 3′ to PGK-neomycin-cassette; o232: 5′-AGAAGATCTGAGAGGGTGCATCCC-3′, antisense primer specific to the loxP-flanked region; o250: 5′-CCCATGCCCAGATCCATGC-3′, sense primer 5′ of left loxP-site. o234: 5′-TGACAGCAATGCTGTTTCACTGG-3′, sense primer specific for Cre-recombinase; o235: 5′-GCATGATCTCCGGTATTGAAACTCC-3′, antisense primer

specific for Cre-recombinase. The thermocycle of the PCR was 35 cycles at 95°C (15s), 68°C (20s), and 70°C (90s).

### Preparation of crude synaptosomal membranes for Western blotting and [$^3$H]glycine uptake

Mice were killed by cervical dislocation and the hippocampal formation as well as the cerebral cortex was rapidly dissected on ice. The tissue was homogenized in 20 volumes of ice-cold 10mM Tris, pH 7.4, 0.32M sucrose and centrifuged for 10min at 1000*g*. The resulting supernatant was centrifuged for 10 min at 27,000 *g* to obtain the crude synaptosomal membranes.

### Western blotting

To determine the impact of forebrain-specific GlyT1 disruption on GlyT1 and NMDAR protein expression, crude synaptosomal membranes derived from two behaviorally naïve 8 weeks old male mutant and two control mice per experiment were re-suspended at a protein concentration of about 2mg/ml, supplemented with an equal volume of 125mM Tris/HCl pH6.8, 20% glycerol, 0.002% bromphenol blue, 10% β-mercaptoethanol, 4% SDS and incubated for 15min at 60°C. Aliquots with increasing protein content (2.5, 5, 7.5, 10, 15, and 20μg) were subjected to SDS-PAGE using 7.5% mini-gels (Mini Protean II, Bio-Rad) and resolved proteins were transferred onto nitrocellulose membranes using a Trans Blot Mini Cell (Bio Rad). The blots were blocked for 1–2h in TBST (10mM Tris/HCl pH8, 0.15M NaCl, 0.05% Tween20) containing 5% non-fat dry milk at room temperature, followed by incubation with affinity purified GlyT1 antiserum (1:1000) (Gabernet et al., 2005) together with a monoclonal antibody directed against the NMDA-NR1 subunit (1:1000, Affinty BioReagents) and a monoclonal antibody directed against β-actin (1:40,000, Chemicon International) overnight at 4°C in TBST/5% blocker. The blots were washed once with 20mM Tris pH7.5, 60mM NaCl, 2mM EDTA, 0.4% SDS, 0.4% Triton-X 100, 0.4% deoxycholate and 3 times with TBST. Incubation with the appropriate HRP-conjugated secondary antibodies was carried out for 1h at room temperature. Following extensive washing immunoreactivity was detected by the enhanced chemoluminescence method (Super Signal West Pico Chemoluminescence, Pierce). Images were captured using a Fuji film LAS-1000 Plus Gel Documentation System, and immunoreactive bands were quantified with the AIDA software (Version 3.25, Raytest, Pforzheim, Germany). Actin immunoreactivity was used to monitor equal sample loading.

### Glycine uptake

Freshly prepared crude synaptosomal membranes derived from two to three behaviorally naïve 8 weeks old male mutant and two to three control mice per experiment were immediately washed twice with 25mM HEPES, pH7.4, 125mM NaCl, 5mM KCl, 2.7mM $CaCl_2$, 1.3mM $MgCl_2$, 10mM glucose (KH buffer) and subjected to [$^3$H]glycine uptake studies. Crude synaptosomal membranes (~100 μg of protein in KH buffer) containing increasing concentrations of unlabeled glycine (5–250μM) were preincubated for 5min at 30°C. Subsequently, 50μl [$^3$H]glycine (0.1μM final concentration; 60Ci/mmol; Perkin-Elmer, Emeryville, CA) in KH buffer was added and uptake was terminated after 15min at 30°C by rapid vacuum filtration using a semiautomatic cell harvester (Skatron Instruments, Lier, Norway). The filters were washed with ice-cold 10mM Tris, pH7.4, 150mM NaCl, dried, and subjected to liquid scintillation counting. Non-specific [$^3$H]glycine uptake was determined in the presence of 10mM glycine, and GlyT1 specific [$^3$H]glycine uptake was measured in the presence of 10μM ALX5407 (Sigma-Aldrich). $V_{max}$ values were determined by nonlinear regression using the GraphPad PRISM 4 software (GraphPad Software, San Diego, CA).

## Electrophysiology

All experiments were performed under blind conditions, and genotypes were determined retrospectively. All subjects were male. There were a total of 13 slice preparations derived from 7 control mice, and a total of 8 slice preparations from 6 mutant mice included in the final analysis. Brains were taken from P21-P30 mice and prepared as described previously (Gabernet et al., 2005). Whole cell patch-clamp techniques were used to study synaptic responses of CA1 pyramidal neurons in response to Schaffer collaterals stimulation delivered via a bipolar stimulating electrode (0.05ms, 1–10V, at 0.1Hz). Whole cell patch-clamp experiments were performed on CA1 pyramidal cells in parasagittal brain slices. After decapitation of the mice, brains were quickly removed and placed in aerated (95% $O_2$, 5% $CO_2$) artificial cerebrospinal fluid (aCSF) solution at 4°C. The aCSF solution was composed of (mM): 124 NaCl, 2.5 KCl, 1.3 $MgCl_2$, 26 $NaHCO_3$, 1.25 $NaH_2PO_4$, 2.5 $CaCl_2$, and 20 glucose. Between experiments the slices were maintained at room temperature of 24°C. Synaptic AMPA responses were evoked from CA1 pyramidal cells every ten seconds with a bipolar platinum electrode and recorded in the voltage clamp configuration with a 4–5 MΩ patch pipette at a holding potential of −60 mV. All experiments were done at room temperature. Baseline recordings were performed with 100mM picrotoxin in the aCSF. With picrotoxin in the recording solution, a surgical cut was made between CA1 and CA3 to prevent the propagation of epileptic discharges between the two subfields. After establishing a stable synaptic response, 20μM NBQX was added to the bath solution; recording then continued for an additional 3 to 4 minutes until the AMPA response was clearly abolished. Any non-AMPA residual current observed during this phase was averaged and subtracted from the averaged synaptic baseline response previously recorded to obtain the values of pure AMPA current for experimental analysis. The holding voltage of the cell was then shifted to +40mV to release the magnesium block of NMDARs and recording continued under the same external stimulus strength as before. Due to the tendency of the NMDA amplitude to decay after reaching a short stable plateau, the maximal response was taken as the index of evoked NMDAR to AMPAR-mediated excitatory postsynaptic currents (eEPSCs). In addition, the ratio of NMDAR/AMPAR-mediated eEPSCs was calculated.

## Behavioral assays

Three separate cohorts of experimentally naïve mice were used for behavioral and cognitive phenotyping. The test sequence, duration of each test, number of rest days between tests, and number of subjects accepted in the final analyses of each test are all summarized in Table 1. The presentation of the behavioral data later will instead follow a logical sequence allowing us to highlight the functional relevance of the findings, and therefore does not necessarily adhere to their chronological sequence. All mice were 11–12 weeks old at the beginning of behavioral testing. They were kept under controlled conditions (21°C at relative humidity of 55%) and a 12/12h reversed light/dark cycle (lights on at 08:00PM). All tests were conducted in the dark phase. The mice were caged in groups of six or less in Macrolon Type-III cages (Techniplast, Milan, Italy), and maintained under ad libitum food and water unless stated otherwise. All housing conditions here were identical to those of our previous study of CamKIIα/Cre-GlyT1-KO mice (Yee et al., 2006) and were conducted in the same laboratory.

All manipulations described here had been approved previously by the Cantonal Veterinary Office of Zurich; they conformed to the ethical standards required by the Swiss Act and Ordinance on Animal Protection and the European Council Directive 86/609/EEC. All behavioral data were subjected to parametric ANOVA of the appropriate design conducted using SPSS for Windows (release 13.0, Chicago, IL). Statistically significant outcomes were further evaluated by restricted ANOVAs whenever appropriate.

**Elevated plus maze—**Unconditioned fear and anxiety related behavior was first evaluated in the elevated plus maze when all animals were behaviorally naive. The maze consisted of

two exposed and two enclosed arms extending from a central square platform. Its construction and dimensions have been fully described elsewhere (Yee et al., 2004). To begin the test, the mouse was gently placed on the central platform with its head facing one of the two opening arms. It was then allowed to explore freely for 5 min before being removed and returned to the home cage. A digital camera connected to a PC running the Ethovision tracking system (Noldus Technology Wageningen, The Netherlands) continuously tracked the animal at a rate of 5Hz. Two anxiety-related measures were computed: (i) percentage of time spent in the open arms = time in open arms/times in all arms × 100%, and (ii) percent number of entries into open arms = entries into open arms/all arm entries × 100%. To index general motor activity level, the cumulative spatial displacement of the animal's center of gravity was also computed.

**Hanging wire test—**Motor response and coordination are potential confounding variables for most behavioral paradigms. These were examined in two standard tests. First, neuromuscular strength was evaluated by the hanging wire test (Crawley, 1996). The apparatus was a rigid wired frame modified from a stainless steel cage top. The frame measured 24 × 29cm, consisted of parallel wires 1.5mm thick, spaced 9.5cm apart (center to center). The wires were exposed only through a central region of 13.7 × 16.5cm so that the mouse could not reach the edges of the frame. The frame was held by a test tube clamp, which in turn was firmly fixed to a metal support stand 40cm above the bench top in a quiet room. The clamp also allowed the frame to be rotated. A layer of sawdust bedding was positioned directly below the frame to allow a soft landing when the animals fell off. At first, the frame was in a horizontal position, and the mouse was placed gently on top of it. The wired frame was then rotated 180° with the mouse now hanging up-side down, and remained so until 5min had elapsed or when the animal fell down. The latency to fall was recorded, and a criterion of 5min was assigned to animals that did not fall.

**Rotarod test—**Motor coordination and motor skills was evaluated using the standard accelerating rotarod apparatus for mice (Model 7650, Ugo Basile, Comerio, VA, Italy). To begin, the mouse was placed on the rotating drum that was turning at the baseline speed of 4rpm. During the 5-min observation period, the speed of rotation increased linearly to 40rpm. A trial ended when the mouse fell from the apparatus or when 5min had elapsed. The latency to fall from the rotating drum was recorded. Animals that did not fall within the time limit were assigned a criterion score of 5min. The animals were tested once per day for three consecutive days, thus further allowing the evaluation of motor skill learning.

**LI of conditioned freezing—**LI is a demonstration of selective learning; it is considered to depend on selective attentional processes sensitive to the associative history of a stimulus (Lubow, 1973; Mackintosh, 1973). It is readily demonstrated in associative learning paradigms whereby non-reinforced pre-exposure of the to-be-conditioned conditioned stimulus (CS) before conditioning leads to a retardation in the development and subsequent expression of a conditioned response to the CS (Lubow and Moore, 1959). In this and all subsequent LI experiments, we adopted a design that, in general, tended to generate weak expression of LI in the control group. This approach is commonly adopted to assess treatments (e.g., antipsychotic drugs) expected to enhance or potentiate LI (Feldon and Weiner, 1991).

The apparatus and procedures have been fully described before (Meyer et al., 2005; Yee et al., 2006). Briefly, there were 8 conditioning chambers equipped with a sonalert to deliver a 30s, $86dB_A$ tone serving as the CS, and a metal grid floor via which a 1s, 0.25mA electric foot shock could be delivered and served as the unconditioned stimulus (US). A digital camera was mounted 30cm directly above the area of interest in each chamber. Successive images captured at 1s intervals were compared to allow the indexation of freezing according to the algorithm described by (Richmond et al., 1998). The pre-exposure and conditioning parameters here followed our previously established protocol (Yee et al., 2006), which led to a marginal LI

effect in the control group. Briefly, the procedure comprised four phases: pre-exposure, conditioning, context test and CS test. Mice of each genotype were randomly subdivided into two conditions: the pre-exposed (PE) and non-pre-exposed (nPE) conditions.

On the first day, PE subjects received 40 presentations of the tone CS at a variable inter-stimulus interval of 40±30s, while nPE subjects were confined to the chamber for an equivalent period of time without any discrete stimulus presentation. Next, the conditioning phase followed immediately without removing the animals from the chambers, and it consisted of three conditioning trials – each began with the tone CS (30s) followed immediately by the shock US (1s). Each trial was preceded and followed by a 180s interval in which no discrete stimuli were presented.

The test of contextual freezing took place 24h later when the subjects were returned to the same chambers and observed for a period of 480s in the absence of any discrete stimulus. The test of conditioned response to the tone CS was conducted another 24h later, when the animals were returned to the same chambers once again. Following an initial acclimatization period lasting 90s, the tone CS was turned on for 480s.

**LI of conditioned active avoidance—**The second associative learning paradigm used to assess LI was ‘conditioned two-way active avoidance’. Signalled conditioned avoidance involves elements of both classical and instrumental conditioning, in which the subjects learn to perform a specific operant act in response to a discrete signal to prevent or avoid the delivery of an aversive foot shock. The apparatus and procedures have been fully described before (Meyer et al., 2005; Yee et al., 2006). Briefly, four identical Coulbourn Instruments two-way shuttle boxes (model H10-11M-SC) were used. Each box comprised two identical compartments separated by a metal wall. An opening (6.5 × 8 cm) in the wall allowed the mouse to shuttle freely between the two compartments. Shuttles were detected by an array of infrared photo sensors positioned on the back wall of the shuttle box. Each box was equipped with a speaker to generate an $83dB_A$ white noise that served as the warning signal and a stainless steel grid floor capable of delivering an electric foot shock at 0.25mA. Again, the procedural parameters were identical to our previous study (Yee et al., 2006) that had enabled the detection of an LI-enhancing effect in forebrain neuron specific GlyT1 conditional knockout mice.

The animals were subdivided into PE and nPE conditions, with their PE/nPE experience in the previous (conditioned freezing) experiment counterbalanced. On the first day, after the animals were placed in the shuttle boxes: the PE subjects received 50 pre-exposures of the noise stimulus (5s, $83dB_A$ in magnitude against a background noise of $63dB_A$) presented at a variable inter-stimulus-interval of 40±15s, and the nPE subjects spent an equivalent period of time in the chamber without any stimulus presentation. On the next day, the animals returned to the shuttle boxes and underwent one hundred conditioned avoidance trials administered at variable inter-trial intervals (ITIs) of 40±15s. A trial began with the onset of the noise stimulus. If the animal shuttled within 5s of stimulus onset, the noise stimulus was terminated and the trial ended without any shock delivery, and the animal had made a successful “avoidance response”. Avoidance failure led immediately to an electric foot shock presented in coincidence to the noise stimulus. During the noise-shock presentation, a shuttle response would terminate both stimuli and the trial ended with the subject scoring an “escape response”. The trial was ended with the termination of both noise and shock if the subjects failed to escape in 2s, and an “escape failure” was scored. Conditioned avoidance learning was indexed by the number of avoidance response across successive 10-trial blocks. Avoidance and escape responses were separately analyzed.

**LI of conditioned taste aversion—**The third associative learning paradigm was ‘conditioned taste aversion’ which is a reliable one-trial classical conditioning paradigm, in

which a single pairing of a taste CS and gastric malaise leads to a long lasting aversion to the taste. Pre-exposure to the taste prior to conditioning would retard the generation of the subsequent conditioned taste aversion response, thereby constituting another method to demonstrate the LI effect. Again, the animals were again either pre-exposed (PE subjects) or not (nPE subjects) to the sucrose solution prior to conditioning. Similar to the two previous two LI experiments, only one pre-exposure was performed to minimize the LI effect in the controls. Here, 10% (w/v) D-sucrose solution served as the taste CS, and gastric malaise induced by an intraperitoneal injection of lithium chloride (LiCl) solution served as the US.

Throughout the experiment, the animals were housed singly in Macrolon cages (1291H, Euro standard type III, Techniplast S.p.a., Milan, Italy) measuring 425 × 266 × 185 mm. After 2 days of habituation to single housing, access to water was gradually restricted over a 5d period as described before (Meyer et al., 2004). On the 5$^{th}$ day, the water restriction was reduced to 1h. Thereafter, and until the end of experiment, the animals were allowed two 30min-drinking periods per day, 4h apart. Two drinking tubes were inserted into the cage in each of the two drinking periods, and the animals could freely consume liquid from either tube as described before (Yee et al., 2006). Manipulations of the content of the drinking tubes were always conducted in the first drinking period of a day. In the second period, both tubes were always filled with plain tap water.

The experimental procedure consisted of four phases: baseline, pre-exposure, conditioning, and test. *Baseline:* Over the first 3 days, both tubes contained water in both drinking periods to acclimatize the animals to drinking from the water tubes. The allocation of subjects into PE and nPE conditions was counterbalanced according to the animals' performance in the first drinking period across the three baseline days. *Pre-exposure:* On the next day, PE subjects were provided with 10 %(w/v) D-sucrose solution in both tubes during the first drinking period, whereas nPE subjects had access to water only in both tubes. *Conditioning:* On the next day, all subjects were provided with sucrose solution in both tubes during the first drinking period, followed 5min later by an intraperitoneal injection of 0.25M LiCl at 2% v/w of the bodyweight. *Test:* On the next day, conditioned taste aversion to the sucrose solution was measured in a two-choice test in which one tube contained sucrose solution and the other water, thus allowing the animals a free choice between the two.

**Water maze—**Next, the water maze was used in two tests of spatial learning. Due to excessive floating exhibited by female mice, these experiments were performed with male mice only. The water maze was a white circular tank made of fiberglass (diameter 102 cm, height 36 cm) filled with water (at 24±1°C) to a depth of 19 cm. Fresh tap water was used on each testing day. A transparent Plexiglas cylinder (diameter 7cm, height 18.5 cm) was used as the escape platform. It was submerged 0.5 cm below the surface of the water, remaining invisible to the animals. It could be made visible by mounting a white circular disk (diameter 12 cm), 15 cm directly above the platform. A digital camera was installed above the water maze, capturing images at a rate of 5 Hz and transmitting them to a PC running the Ethovision (Noldus Technology) tracking system. Ethovision computed the escape latency, distance travelled (i.e., path length), and average swim speed on each trial, and the additional dependent measures on probe tests in the reference memory task (see below). The water maze could be positioned in the center of one of two possible well-illuminated testing rooms (referred to as Room 1 and Room 2), each enriched with unique distal spatial cues. The pre-training phase and the working memory experiment were conducted in Room 1, and the reference memory experiment in Room 2.

**Cued Test (Day 1):** On the first day, the animals were pre-trained using a cued (i.e., visible) platform located in the centre of the maze in order to familiarize them to the apparatus and to swimming in the pool. It further served as a test of any non-specific sensory and motor

disturbance. The platform was positioned in the center of the maze. Each animal underwent two consecutive trials. The starting position varied randomly among four possible release points (N, E, S, and W). To begin a trial, the subject was gently released from the start point, facing the wall of the maze. The animals were allowed to locate the escape platform within 60s. Upon reaching the platform they spent an ITI of 15s on it before the second trial commenced. If an animal failed to locate the platform within the time limit of 60s, it was guided to the platform by the experimenter and allowed to stay on it for 15s, and a maximal escape latency of 60s was scored.

**Working Memory (Days 2–28):** The working memory task was based on the matching-to-sample paradigm, in which the animals were required to learn the novel position of the platform revealed to them on trial 1 of each day in order to navigate effectively to the same location (i.e., matching) on subsequent trials on the same day (Hodges et al., 1995). The daily change of platform location ensured that the solution on a given day was irrelevant for the next day, thus taxing the flexible use of (short-term) working memory. The procedures were similar to the cued test, except that the platform was now hidden from the animals' view and assumed a novel location on each day, but remained in that position from trial 1 to 2. In all trials, the animals were allowed a maximum of 60s to locate the platform, upon then it would be guided to the platform by the experimenter.

To manipulate the retention demand of the task in the temporal domain, the ITI between trials 1 and 2 was also varied. First, the minimal ITI of 15s was employed – this referred to the time animals spent on the platform at the end of trial 1 to the beginning of trial 2. This lasted for six days. Following a break of one day, the ITI was increased to 10min over the next six days. This was followed by another six days with an ITI of 15min, and then a final six days with again an ITI of 10 min. During the extended ITIs of 10 or 15min, the animals spent the first 15s on the platform, and the remaining time in an opaque waiting box located in the testing room.

The six platform locations used in the first six days with the minimal ITI were: 35 cm off center in the NE, SW and NW directions, and 15 cm off center in the N, E and S directions. Across subsequent days, a total of 16 platform locations were defined. These were located at either 15 cm or 35 cm away from the center in the following eight directions: N, E, S, W, NE, NW, SE and SW directions. All positions were used once only in every 16 trials, and then a new random sequence was generated. The start positions also varied between trails among eight possible release points along the maze wall: N, E, S, W, NE, NW, SE and SW. Each animal followed its own unique random non-repetitive sequence; and a new sequence was generated for every block of 8 trials.

**Reference memory learning and its reversal (Days 33–46):** Reference memory learning was conducted in another testing room, and commenced seven days following the working memory test. The initial acquisition lasted for 8 days, with 4 trials per day and an ITI of 15s. The escape platform was positioned 25 cm from the maze center in one of the four quadrants – the target quadrant. Assignment of the target quadrant was counterbalanced, so that all four quadrants were used in each group. The start position varied among eight possible release points (N, E, S, W, NE, NW, SE and SW), and was determined as described above. A probe test was conducted prior to reference memory training on the eighth acquisition day. During a probe test, the platform was removed and the animals were allowed to swim freely in the maze for 45s after being released from the point opposite to the target quadrant. The time and distance spent in each of the four quadrants were subjected to analysis for search accuracy. Reversal testing began on the next day as described above except that the platform was moved to the opposite quadrant. Following 4 days of reversal learning, another probe test was performed on the following day as described above.

**Object recognition memory—**This serves as a non-spatial memory test. The apparatus consisted of a rectangular arena measuring 40 × 61 cm and was surrounded by 22 cm high transparent Plexiglas walls (Singer et al., 2007). An outer perimeter wall of white opaque Plexiglas was positioned 15 cm around the entire arena to minimize interference by extra-maze cues. The arena was divided into three equal compartments by the addition of two partition walls. Each wall had a circular opening (5 cm in diameter) in the middle, positioned at 1 cm above the floor of the arena providing access to the side compartments from the central compartment. The circular opening could be blocked by a Plexiglas sliding door. A collection of distinct three-dimensional objects (in triplicates) differing in form, size, texture, materials and smell served as trial-unique discriminanda. A digital camera was mounted directly above the arena. Video records of all sessions were stored for subsequent data extraction. Prior to object recognition tests, the animals were first habituated to the arena for two days as described by Singer et al. (2007).

An object recognition trial comprised a sample phase and a test phase. To begin the mouse was placed in the middle compartment and two copies of the to-be-familiarized objects (A1 and A2) were positioned in the middle of the two side compartments. First, access to one compartment was closed, and the animal was allowed to explore object A1 (in the center of the accessible compartment) for 5min. Next, the animal was again placed in the central compartment, and it was allowed to explore object A2 (located in the center of the other side compartment) for 5 min by closing the door to the compartment containing object A1. This completed the sample phase and the animals was removed from the arena and kept in a holding cage for the retention interval (2min or 2h), except for retention of 1day when the animals were return to the home cage. Before commencement of the choice phase, the arena was cleansed with 50% ethanol and dried. In the test phase, access to both compartments was available. One compartment contained a third copy of the sample object (A3), and the other a novel object (B). The relative placement of the two objects was counterbalanced across subjects at each retention condition. The animal was allowed to explore freely for 5min.

Only one trial was performed in a day. A total of six object trials were run, spanning across a period of 13 days, with a 24h test-free period separating consecutive trials. On days 1 and 3, the retention interval was 2min. On days 5 and 7, the retention interval was 2h. On days 9–10 and 12–13, the retention interval was 1day. All trials were conducted in the same testing room, and a fresh set of objects was used for each trial.

Object exploration was collected manually by an experimenter who was blind to all conditions (grouping and object identities) with the assistance of Noldus Observer®. Object exploration was defined as active interaction of the animal (e.g., sniffing, gnawing) with the object at a distance of less than 1 cm (Singer et al., 2007). Object recognition was not scored when an animal made a contact with the objects without facing it, or when it climbed on top of the objects. Data collected from the sample and test phases were separately analyzed because the amount of exploration directed towards the sample objects in the familiarization phase constitutes a critical variable as it is expected to influence the animals' familiarity judgment in the test phase (Singer et al., 2007). It is therefore imperative to examine whether the mutation alters exploration behavior as such. In the test phase, preferential exploration of the novel over the familiar object was taken as a measure of object recognition relying on the natural tendency of rodents to explore novel elements in their environment. In addition, a discrimination ratio based on exploration time was calculated: (novel − sample)/(novel + sample), to index the preferential exploration of the novel objects as suggested by Aggleton (1993) whereby a positive ratio indicates a preference for the novel object. Data across two trials of the same retention condition were averaged before being submitted to statistical analysis.

**Locomotor response to acute systemic PCP or amphetamine challenge—**The NMDAR antagonist PCP and the dopamine releaser amphetamine are psychoactive drugs which have been found to induce hyperactivity at the given doses in the littermate controls of the forebrain neuronal GlyT1 knockouts (Yee et al., 2006). Changes in GlyT1 function is expected to alter the acute response to these psychostimulants (Depoortere et al., 2005; Yee et al., 2006; Singer et al., 2009a).

Motor activity was measured using four white open fields measuring (40 × 40 cm) as described before (Hauser et al., 2005). A digital camera mounted above the open fields captured images at a rate of 5 Hz and transmitted them to a PC running the Ethovision tracking system (Noldus Technology), which calculated a mobility score defined as cumulative displacement of the animal's centre of gravity in successive 10-min bins.

The motor response to PCP was tested using a between subject design: the mice were injected with 5 mg/kg PCP or vehicle saline solution (0.9% NaCl) via the intraperitoneal route (at an injection volume of 5 ml/kg) immediately before being put inside the open field, and observed for 1h. Following one week of washout period, the reaction to systemic amphetamine (2.5mg/kg, i.p.) was assessed in the same animals, with previous drug or vehicle experience counterbalanced. Again, animals were injected with amphetamine (2.5 mg/kg, i.p.) or vehicle saline solution (0.9% NaCl) immediately before the test, and were observed for an extended period of 90min.

## RESULTS

### Deficient GlyT1- but not NMDAR-expression in the forebrain of *EMX/GlyT1-KO* mice leads to reduced glycine-re-uptake

The expression of GlyT1 protein levels in mutant mice was substantially reduced. At high protein concentrations, faint GlyT1 immunoreactivity was detectable in mutant mice, whereas samples from control mice showed intense signals (Fig. 1A). Quantification of the blots to the GlyT1 protein signal intensity at 20 micrograms in controls (100%) revealed a 79±2% (±SEM, n=4) reduction of GlyT1 protein levels in mutant as compared to control mice (Fig. 1B). This confirms the efficacy of the mutation to significantly reduce GlyT1 protein expression in the hippocampus/cortex of mutant mice. The functional consequence of the reduced GlyT1 protein levels was assessed in [$^3$H]glycine uptake studies. As expected from the strongly diminished protein levels, GlyT1-specific [$^3$H]glycine uptake was likewise reduced by 77±1% in mutant mice (Fig. 1D; control: $K_M$ = 72±16 μM; $V_{max}$ = 79±22 pmol/min/mg protein, mutant: $K_M$ = 20±2 μM; $V_{max}$ = 18±0.7 pmol/min/mg prot.; ±SEM, n=3). These results indicate that GlyT1 protein levels and GlyT1-specific glycine uptake were affected to a similar extent in mutant mice. On the other hand, Western blot analysis using NMDA-R1 specific antibodies revealed that the mutation did not alter NMDAR protein expression (Fig. 1C).

### The reduction in GlyT1-mediated glycine reuptake in *EMX/GlyT1-KO* mice does not affect NMDAR-mediated neurotransmission

The ratio of the peak amplitudes of NMDAR to AMPAR-mediated EPSCs did not significantly differ between mutant [mean±SEM=0.64±0.09] and control mice [mean±SEM=0.56±0.08] (see Fig. 2A). Analysis indicated that the slight difference between the two ratios was far from statistical significance [F(1,11)=0.41, p=0.54]. To ensure that the lack of difference in the NMDAR to AMPAR-mediated EPSCs ratio was not associated with parallel shift in both NMDAR to AMPAR components, the average peak amplitude of evoked AMPAR and NMDAR-mediated eEPSCs were also separately analysed (Fig. 2B–C), which also failed to reveal any statistically significant difference between groups.

### The motor stimulant effect of PCP, but not of amphetamine, is attenuated in *EMX/GlyT1-KO* mice

As illustrated in Fig. 3A, systemic PCP (5mg/kg, i.p.) injection led to an immediate increase in activity in control mice over 3-fold of that seen following saline injection, which subsided by the end of the 60-min observation period. The motor stimulant effect of PCP was, however, substantially reduced in the mutant mice. This drug-induced phenotype was observed in both male and female mutants. Furthermore, female generally were more active than male mice (data not shown). A 2 × 2 × 2 × 6 (genotype × sex × drug × 10-min bins) ANOVA of distance moved per bin confirmed the above impressions in revealing a significant main effect of sex [$F(1,28)=20.87$, $p<0.001$] and a highly significant genotype × drug × bins interaction [$F(5,140)=4.79$, $p<0.001$]. The latter interaction indicated that the drug's effect on locomotor activity over time in comparison to saline vehicle injection significantly differed between mutant and control groups. This three-way interaction was further accompanied by a highly significant effect of drug [$F(1,28)=22.54$, $p<0.001$], bins [$F(5,140)=7.61$, $p<0.001$], and their interaction [$F(5,140)=9.48$, $p<0.001$]. Further analyses restricted to either injection condition confirmed that mutant and control mice did not significantly differ under saline condition: neither the genotype effect nor its interaction was close to significance. In contrast, the analysis restricted to the PCP condition yielded a clear genotype by bins interaction [$F(5,70)=6.80$, $p<0.005$], which was further accompanied by a near-significant main effect of genotype [$F(1.14)=3.95$, $p=0.067$] indicating that the two genotypes only differed in the PCP condition. This clearly demonstrates that the EMX/GlyT1-KO was behaviorally effective against blockade of NMDAR achieved by PCP.

In contrast, the response to amphetamine appeared to be highly comparable between groups (Fig. 3B). Amphetamine led to a drastic increase in locomotor activity in both groups, reaching a peak at 30min into the test. By the end of the 90-min observation period, the motor stimulant effect had largely subsided. A 2 × 2 × 2 × 9 (genotype × sex × drug × 10-min bins) ANOVA of distance moved per bin yielded a main effect of drug $F(1,28)=79.96$, $p<0.001$] and its interaction with bins [$F(8,224)=32.53$, $p<0.001$]. Similar to the PCP experiment, a main effect of sex emerged [$F(1,28)=10.10$, $p<0.005$], because female mice again were generally more active than male (data not shown). There was no statistical evidence for any difference between genotypes.

Although the animals used in test of amphetamine-induced hyperactivity here were not drug naïve, we have since repeated the experiment with completely naïve animals, and have obtained the same null effect in the EMX/GlyT1-KO mice (data not shown).

### *EMX/GlyT1-KO* mice show a delay-dependent facilitation in object recognition memory

**Sample phase—**Mutant and control mice spent a similar amount of time exploring the sample objects in the sample phase across the different delay conditions However, male mice tended to spend more time in sample exploration than female mice. This was in line with a 2 × 2 × 3 (genotype × sex × delays) ANOVA of object exploration time per sample run yielding only a significant main effect of sex [$F(1,30)=25.14$, $p<0.001$]. The mean exploration time (in sec, ±SEM) per sample run collapsed across all delay conditions was: ♂control=21.44±2.49, ♂mutant=23.43±2.87; ♀control=8.64±1.16, ♀mutant=11.21±1.73. From this it follows that a potential effect of the mutation on object recognition memory cannot be attributed to changes in the object familiarization phase.

**Test phase—**As illustrated in Fig. 4A, both mutants and controls exhibited a clear and comparable preference towards the novel over the familiar object when the delay from sample to test phase was 2min,, as indexed by a positive discrimination ratio. When the delay was increased to 2h, a preference for the novel object remained detectable in the mutant mice but

not in the controls. At 24h delay, both groups were essentially indifferent between the novel and familiar objects. Despite the sex difference observed in the sample phase, sex did not affect performance in the test phase, and the mutation's effect on object recognition was similarly observed in both sexes. The above impressions were supported by the emergence of a significant main effect of genotype [$F(1,30)=4.32$, $p<0.05$] and delays [$F(2,60)=6.20$, $p<0.005$] as well as their interaction [$F(2,60)=6.93$ $p<0.005$] from a 2 × 2 × 3 (genotype × sex × delays) ANOVA of the discrimination ratio. Further analyses restricted to each delay condition indicated that mutant and control mice differed significantly at 2h delay [$F(1,30)=17.30$, $p<0.001$], but not in the shorter or longer delay [$Fs<1$]. The delay-dependency of this phenotype is suggestive of a specific enhancement in memory retention.

The observed enhancement in novelty preference above based on the analysis of discrimination ratio may either be attributed to enhanced exploration of the novel objects (i.e., 'enhanced novelty detection') or reduced exploration of the familiar objects (i.e., "reduced forgetting"). We attempted to discriminate between the two possibilities by directly comparing the exploration times towards the novel and familiar objects in the test phase. As shown in Fig. 4B, the control and mutant mice did not differ in their exploration time to the familiar object in the critical 2h delay condition, whilst the mutant spent considerably more time exploring the novel object. This lends support to the conclusion that the enhanced object recognition performance by the mutant reflects primarily superior novelty detection, rather than reduced forgetting. This conclusion was confirmed by a 2 × 2 × 3 × 2 (genotype × sex × delays × objects) ANOVA yielding a critical genotype × delays × objects interaction [$F(2,60)=4.73$, $p<0.05$], which is in complete agreement with the impression of the discrimination ratio analysis described above. Supplementary restricted analyses revealed that a statistically significant genotype × objects interaction was only revealed in the 2-h delay condition [$F(1,30)=9.84$, $p<0.005$]. This is attributed to the presence of a significant novelty preference in the mutant [$p<0.05$], but not in the controls.

### *EMX/GlyT1-KO* mice exhibited enhanced spatial working memory in the water maze

**Cued (visible platform) task—**All animals acquired the swimming response and learned to escape onto the platform. Performance in both latency and distance to escape was comparable between groups. Parallel 2 × 2 (genotype × trials) ANOVA of the escape latency and the path length yielded only a significant effect of trials [escape latency: $F(1,16)=17.18$, $p=0.001$; path length: $F(1,16)=24.20$, $p<0.001$]. The mean (±SEM) escape latency across the two trials was as follows: control: trial 1 = 44.3±7.9s, trial 2 = 22.6± 6.4s, and mutant: trial 1 = 40.9±7.1s, trial 2 = 18.2±4.6s. The corresponding values for the path length were: control: trial 1 = 766.5 ±158.9cm, trial 2 = 334.0±93.8s, and mutant: trial 1 = 840.0±142.2s, trial 2 = 295.7±83.9s. Separate analysis of swim speed did not reveal any effect of genotype or its interaction.

**Working memory—**First, to assess whether the two groups of mice were able to learn the matching rule underlying the working memory task, working memory was assessed under minimal retention demand with a 15s ITI separating trial 1 and 2. Escape latency and path length were subjected to separate 2 × 6 × 2 (genotype × days × trials) ANOVAs. Mutant and control mice showed comparable overall improvement form trial 1 to 2 (see summary portion of Fig. 5A and 5C), suggesting that both groups had acquired the matching rule underlying this spatial working memory task, to reach the platform effectively on trial 2 based on information acquired on trial 1. This impression was supported by the emergence of a significant main effect of trials [escape latency: $F(1,16)=23.68$, $p<0.001$; path length: $F(1,16)=13.86$, $p<0.005$] in both measures. Performance also showed some variation across days [escape latency: $F(5,80)=6.37$, $p<0.005$; path length: $F(5,80)=6.23$, $p<0.005$], but there was no statistical evidence for a days by trials interaction. Neither the effect of genotype nor any of its interactions reached statistical significance, in spite of the faster swim speed of mutant mice [$F(1,16)=6.02$,

p<0.05]. The mean swim speed (in cm/s) was as follows (±SEM): control=16.8±1.0, mutant=19.5±0.5.

Next, the temporal retention demand was increased by extending the ITI between trials 1 and 2. Over 18 days, the ITI was extended to 10min in the first block of 6 days, then to 15min in the next block, and returned to 10min in the final blocks.

Escape latency and path length were separately conducted using a 2 × 3 × 6 × 2 (genotype × blocks × days × trials) ANOVA design. The analyses yielded no indication of differences amongst blocks (10-min vs. 15-min vs. 10-min). As illustrated in the summary portion of Fig. 5B and **5D**, the overall improvement from trials 1 to trials 2 was more prominent in the mutants than controls in both performance measures. This gave rise to a significant main effect of trials [escape latency: $F(1,16)=9.80$, $p<0.01$; path length: $F(1,16)=16.38$, $p<0.001$] and its interaction with genotype [escape latency: $F(10,160)=4.39$, $p=0.001$; path length: $F(10,160)=4.43$, $p=0.001$]. Additional analyses restricted to either mutant or control groups confirmed that the emergence of the significant genotype by trials interaction stemmed from the presence of a significant trials effect in the mutant mice [escape latency: $F(1,9)=22.64$, $p<0.005$; path length: $F(1,9)=25.91$, $p<0.005$], but not in the control group [$Fs<1$].

Although overall performance did not differ across blocks, significant daily variation within blocks was observed [escape latency: $F(5,80)=13.18$, $p<0.001$; path length: $F(5,80)=13.39$, $p<0.001$]. The improvement in performance across days was most pronounced in the first block, but gradually weakened in subsequent blocks (Fig. 5B and 5D), leading to the emergence of a blocks by days interaction [escape latency: $F(10,160)=4.39$, $p<0.001$; path length: $F(10,160)=4.43$, $p<0.001$]. However, neither the factor blocks nor days showed any significant interaction with the factor trials.

When variation across days was present, there is a possibility that the trials effect may also capture the reference memory component of the task (e.g., the delayed matching-to-position rule). We have examined that the specific contrast between trials 1 to 2 within days reflects working memory function, because the contrast between trials 2 (day N) and trial 1 (day N+1) did not revealed any significant effects.

Separate analysis of swim speed again suggested that mutant mice were swimming marginally faster [$F(1,16)=3.98$, $p= 0.06$]. The mean (±SEM) swim speed (in cm/s) across the three blocks was: control=15.8±1.2, mutant=18.2±0.5. An additional analysis of covariance (ANCOVA) with swim speed as covariate was therefore performed to assess the impact of the statistical outcome in escape latency described above. The critical genotype × trials interaction remained significant [$F(1,15)=7.28$, $p<0.05$], and the effect of covariate did not reach statistical significance [$F(1,15)=2.86$, $p=0.11$]. The possibility that the mutation's effect on working memory performance stems solely from an increase in swim speed is therefore highly unlikely, especially when the results of path length closely conformed to the results based on escape latency.

One may speculate that enhanced working memory performance in the mutant mice might be associated with a reduced susceptibility to proactive interference from memory trace of the platform location of the previous day. This possibility can be addressed by additional analysis of the existing data set. To this end, we focused on the search path obtained on the first trial of a given day (day N) and examined if it exhibited a tendency to return to the vicinity of the platform location on the previous day (day N−1). This was achieved by defining a target zone measuring 14 cm in diameter centred on the platform (7 cm in diameter) location of the previous day, to allow the derivation of the following two variables: percent time spent in this zone, and percent path length recorded in this zone. They were normalized (and therefore expressed in percent) with respect to the escape latency and total path length recorded on the respective

trial. These analyses included the first trial of every test day that followed a day of working memory training 24h before (therefore, the first day of each block was not included). The block of training under minimal delays (15s) and the three blocks of extended delays (10 or 15min) were separately analysed. The data indicated that the mice indeed showed a tendency to return to the vicinity of the former platform location (target zone) beyond that expected by chance. During the block of training under minimal ITI, the control mice devoted 3.78±0.66% of time and 3.97±0.70% of the total path length to the target zone; the corresponding values for the mutants were 4.18±0.59% and 4.71±0.63%, respectively. These are all above the value of 1.88% expected by chance alone [$p<0.05$]. This tendency was even more pronounced when the ITI delay was extended [percent time in the target zone: control=7.53±1.11%, mutant=6.23 ±0.99%; percent path length in the target zone: control=10.79±1.48%, mutant=7.95±1.32%]. However, there was no statistical evidence for any genotype difference in these additional analyses.

### *EMX/GlyT1-KO* mice display normal acquisition of spatial reference memory and reversal learning

Acquisition of the task developed progressively over the eight days of training as indicated by a reduction in escape latency and path length as a function of days (Fig. 6A–6B). The acquisition rate was similar between mutant and control mice. Within a day, the performance generally improved across trials. Separate 2 × 8 × 4 (genotype × days × trials) ANOVAs of the escape latency and path length both yielded a highly significant effect of days [escape latency: $F(7,112)=6.95$, $p<0.001$; path length: $F(7,112)=8.42$, $p<0.001$] and trials [escape latency: $F(3,48)=4.98$, $p<0.005$; path length: $F(3,48)=4.35$, $p<0.01$]. Consistent with the impression above, neither the main effect of genotype nor its interactions attained statistical significance. Moreover, mutant and control mice no longer differed in swim speed [$F(1,16) =1.82$, $p=0.196$]. The mean (±SEM) swim speed (cm/s) was: control=15.4±1.2, mutant=18.2 ±1.7].

At the beginning of the reversal phase, performance was drastically reduced in all animals (Fig. 6A–6B). However, they quickly adapted to the change and by the fourth day had achieved a rapid escape to the platform. There was no apparent difference between groups as indicated by separate 2 × 4 × 4 (genotype × days × trials) ANOVAs of the escape latency and path length, which yielded only a main effect of days [escape latency: $F(3,48)=18.34$, $p<0.001$; path length: $F(3,48)=17.83$, $p<0.001$]. Furthermore, the animals' performance generally improved over trials [escape latency: $F(3,48)=8.14$, $p=0.001$; path length: $F(3,48)=8.06$, $p<0.001$]. No significant difference in swim speed was observed [$F<1$]. The mean (±SEM) swim speed (cm/s) was: control=16.5±1.4, mutant=17.8±1.0].

Two probe tests were conducted: 24h after acquisition training, and likewise after reversal learning. These allowed an evaluation of spatial search in the absence of the platform. The results were consistent with the above analyses that no difference between groups was apparent. As illustrated in Fig. 6C, both mutant and control mice showed a clear bias in their search in the target quadrant, well above the chance level performance, in the probe test following acquisition training. At the same time, they also avoided in particular the opposite quadrant. A 2 × 4 (genotype × quadrants) ANOVA of percent time spent per quadrant of the first probe test yielded only a highly significant effect of quadrants [$F(3,48)=27.79$, $p<0.001$], and similarly so when percent path length per quadrant was analyzed [$F(3,48)=27.03$, $p<0.001$] (data not shown). In the second probe test, the spatial distribution of search behavior was again highly similar between groups (Fig. 6D). However, the bias towards the new target quadrant was less pronounced, and there was not a tendency to avoid the opposite (former target) quadrant. Again, the analysis yielded a highly significant quadrants effect [percent time per quadrant: $F(3,48)=,10.97$ $p<0.001$; percent path length per quadrant: $F(3,48)=11.89$, $p<0.001$].

These results suggested that the mutation affected neither the acquisition nor the retention of spatial reference memory.

## Neither associative learning nor LI was potentiated in the EMX/GlyT1-KO mice

**Conditioned Freezing—**First, associative learning was assessed using the conditioned freezing paradigm with or without prior CS pre-exposure. Conditioning took place immediately following CS pre-exposure (PE subjects) or context pre-exposure (nPE subjects). Over the three trials of tone-shock pairings, an increase in freezing to the CS tone was observed in all groups (Fig. 7A). However, the rate of increase was retarded in the PE subjects relative to the nPE subjects, constituting the LI effect. This was similarly seen in both mutant and control mice. These impressions were confirmed by a 2 × 2 × 2 × 3 (genotype × pre-exposure × sex × trials) ANOVA of percent time freezing which yielded a significant effect of trials [$F(2,64)=37.36$, $p<0.001$] and of pre-exposure [$F(1,31)=5.10$, $p<0.05$]. No other effect attained statistical significance. Next, the conditioned freezing developed to the context was assessed by returning the animals to the conditioning chamber 24h following tone-shock pairing. As illustrated in Fig. 7B, the expression of conditioned freezing over the 480s test period was comparable across groups. A 2 × 2 × 2 × 8 (genotype × pre-exposure × sex × 1-min bins) ANOVA of percent time freezing yielded only a significant main effect of bins $F(7,224)=3.44$, $p<0.01$]. Another 24h later, conditioned freezing to the CS was evaluated. Ninety seconds after the animals returned to the conditioning chamber, the CS was turned on continuously for 480s and the expression of freezing in response to the CS was examined (see Fig. 7C). In both mutant and control mice, nPE subjects exhibited somewhat higher levels of freezing than PE subjects. This difference diminished over time as the overall levels of freezing gradually reduced due to extinction. A 4-way 2 × 2 × 2 × 8 (genotype × pre-exposure × sex × 1-min bins) ANOVA of percent time freezing per bins yielded a significant main effect of bins [$F(7,224)=33.67$, $p<0.001$] and a significant pre-exposure by bins interaction [$F(7,224)=3.52$, $p<0.05$]. Restricted analyses indicated that the presence of a main pre-exposure effect only in the first bin [$F(1,32)=15.94$, $p<0.001$]. There was no statistical evidence for any difference between groups – either in the magnitude of conditioned freezing or the expression of the LI effect.

**Conditioned active avoidance—**In the pre-exposure phase, PE subjects exhibited somewhat less spontaneous shuttles than nPE subjects in both mutant and control mice [PE: control=43.3±5.4, mutant=47.6±9.8; nPE: control=57.5±8.0, mutant=71.8±10.6]. A 2 × 2 × 2 (genotype × pre-exposure × sex) ANOVA of total spontaneous shuttles yielded a main effect of pre-exposure that just failed to attain significance [$F(1,33)=4.00$, $p=0.05$]. Active avoidance learning was indexed by number of avoided trials over successive 10-trial blocks (Fig. 8). All groups exhibited a similar increase over blocks reaching asymptotic level by the second half of the session. Neither genotype nor pre-exposure condition appeared to affect the rate of conditioned avoidance learning. These impressions were confirmed by a 2 × 2 × 2 × 10 (genotype × pre-exposure × sex × 10-trial blocks) ANOVA, which only yielded a significant main effect of blocks [$F(9,297)=92.60$, $p<0.001$]. Despite the absence of an overall LI effect, the results of this experiment are in agreement with the previous conditioned freezing experiment: the mutation did not enhance avoidance learning as such, nor did it lead to the expression of LI under conditions insufficient to generate LI in control mice.

**Conditioned taste aversion—**As expected, consumption of liquid in the pre-exposure phase was higher in the PE than nPE subjects due to the rewarding taste of sucrose in the pre-exposure phase (Table 2). A 2 × 2 × 2 (genotype × sex × pre-exposure) ANOVA of liquid consumption during pre-exposure session yielded a significant effect of pre-exposure [$F(1,38)=21.14$, $p<0.001$]. Conditioning took place 24h later, and it was uneventful (Table 2). A similar analysis of liquid consumption yielded no significant outcome. In the conditioned taste aversion test on the next day, aversion was indexed by percent consumption of sucrose solution.

LI was evident by increased aversion in the nPE relative to the PE subjects. This was largely similar in both mutant and control mice (Fig. 9). A 3-way ANOVA (genotype × sex × pre-exposure) ANOVA of percent consumption of sucrose solution confirmed the overall presence of LI by yielding a significant pre-exposure effect [$F(1,38)=5.43$, $p<0.05$]. Neither the main effect of genotype nor its interaction attained statistical significance. Additional analysis of total liquid consumption (water *plus* sucrose solution) did not yield any significant effects **(**Table 2). These results provided further support to the conclusion of the previous two associative learning experiments that neither conditioning as such nor LI expression differed significantly between mutant and control mice.

## Normal anxiety-like behavior in *EMX/GlyT1-KO* mice

Mutant and control mice were comparable in both anxiety measures: % time in open arms (control = 27.6±5.7%, mutant = 35.7±8.0%) and % open arms entries (control = 37.2±4.7%, mutant = 35.0±6.7%). They also did not differ in terms of locomotor activity in the elevated plus maze based on the measure of cumulative distance travelled [control = 7.55±0.50m, mutant = 7.24±0.60m]. Separate 2 × 2 (genotype × sex) ANOVAs of all three measures failed to yield any significant effect.

Hence, the behavioral outcomes reported above are not confounded by changes in potential change in emotionality in the form of anxiety or generalized fear to aversive environmental stimulus.

## Normal sensory motor coordination in *EMX/GlyT1-KO* mice

**Hanging wire test—**As illustrated in Fig. 10A, the latency to fall from the hanging wire was highly comparable between mutant and control mice, although male mice [52.8±6.6s] were in general performing poorer than female [289.3±10.4s]. A 2 × 2 (genotype × sex) ANOVA of the latency to fall (in sec) yielded only a main effect of sex [$F(1,37)=341.90$, $p<0.001$]. Because of the significant difference in body weight between sexes [♀ control=28.0±0.7g, ♀ mutant=28.2±0.6g, ♂ control=38.7±0.7g, ♂ mutant: 39.5±0.9g)], which may exert a confounding effect on the latency measure, an additional ANCOVA was performed with body weight as covariate. However, the main effect of sex remained statistically significant [$F(1,36) = 69.90$, $p < 0.001$]. Hence, it is unlikely that the sex difference observed in the hanging wire test could be solely attributed to body between-sex weight difference.

**Accelerating Rotarod—**The latency to fall increased over days in both groups (Fig. 10B), but again the two groups did not differ significant from each other. Again, a sex difference, independent of genotype, was observed: male mice fell earlier than female mice, although this difference disappeared by the third test day. These impressions were confirmed by a 2 × 2 × 3 (genotype × sex × days) ANOVA of the latency to fall (in sec), which yielded a main effect of days [$F(2,74)=13.27$, $p<0.005$], of sex [$F(1,37)=6.50$, $p<0.02$], and their interaction [$F(2,74)= 5.33$, $p<0.01$]. No other main effect, including the genotype effect or interaction terms attained statistical significance. As previously, additional analysis of covariance (ANCOVA) was performed on the mean latency to fall across the three days with body weight as the covariate. The ANCOVA indicated that the main effect of sex was no longer significant [$F<1$], suggesting that the observed difference between sexes could be statistically accounted for by individual differences in body weight.

Therefore, the cognitive effects of the mutation reported above cannot be attributed to possible confounding changes in general motor function or coordination.

## DISCUSSION

GlyT1 has emerged as a promising pharmacological target to treat cognitive dysfunctions in schizophrenia or to enhance general cognition function (Atkinson et al., 2001; Gadea and Lopez-Colome, 2001; Chen et al., 2003). Following the discovery of neuronal GlyT1 (Cubelos et al., 2005), the cell-type specific roles of GlyT1 (neuronal *vs.* glial) in modifying cognitive functions have not been addressed. Development of GlyT1-inhibitors for clinical application depends on a more thorough understanding of the cell-type specific roles of GlyT1 in regulating cognitive functions. Previous genetic models were based on heterozygousity of GlyT1 (50% reduction of GlyT1 in neurons and astrocytes) providing a general model of reduced GlyT1 function (Gomeza et al., 2003; Tsai et al., 2004; Martina et al., 2005), or forebrain-selective deletion of GlyT1 in neurons (Yee et al., 2006), designed to exert a more selective effect on NMDAR functions However, non-selective pharmacological treatment would imply blockade of GlyT1-mediated glycine transport in neurons as well as astrocytes. It is therefore imperative to study GlyT1 function in an animal model, in which GlyT1 has been deleted in both cell types. Since homozygous global deletion of GlyT1 is lethal (Gomeza et al., 2003), we decided to knockout GlyT1 specifically in neurons and astrocytes of the forebrain (EMX/GlyT1-KO). Biochemical analysis of EMX/GlyT1-KO mice confirmed that the resulting GlyT1-deficiency in forebrain was associated with a clear disruption in glycine re-uptake.

### EMX/GlyT1-KO confers a resistance to acute PCP challenge in the absence of enhanced NMDAR-mediated currents

A direct consequence of forebrain-selective (in neurons and glia) GlyT1 disruption was the near-complete absence of response to the acute PCP challenge. This suggests that NMDAR function in EMX/GlyT1-KO mice, was altered – being more resistant to systemic pharmacological blockade, presumably due to increased levels of synaptic glycine. This is in keeping with the robust finding that GlyT1 inhibitors is highly effective in attenuating the motor stimulant effect of NMDAR blockers (Harsing et al., 2003; Depoortere et al., 2005; Boulay et al., 2008; Singer et al., 2009a). The lack of an effect on NMDAR- or AMPAR-evoked EPSCs in the hippocampus of EMX/GlyT1-KO mice indicates that the resistance to the PCP challenge does not necessarily require increased hippocampal NMDAR-mediated currents. Since NMDAR-mediated EPSCs were not tested under challenged conditions (e.g. by a low dose of PCP), we cannot entirely exclude the possibility that the effect of the GlyT1 knockout was masked by a ceiling effect. Nonetheless, this seems unlikely because the more restricted forebrain neuron-specific GlyT1 knockouts was clearly associated with a selective elevation of NMDA (but not AMPA) currents when evaluated under the same conditions, when comparing to controls that were genetically identical to those in the present study (Yee et al., 2006). Therefore, the altered response to PCP observed in the EMX/GlyT1-KO mice might still be linked to a selective enhancement of NMDAR-mediated EPSC.

Reduced GlyT1 expression and the resulting elevation of extracellular glycine is not only highly effective in enhancing glycine-B site occupancy, but can also lead to other cellular events, which in turn may affect NMDAR function at the network level in different directions. Thus, it has been shown that pharmacological blockade of GlyT1 can enhance as well as impair NMDAR function. Martina et al. (2004) reported that NMDAR-mediated currents were significantly enhanced in the presence of 25nM of the GlyT1 inhibitor CP802079, but were reduced at higher concentrations (50–1000nM). These authors attributed the latter negative impact on NMDAR-mediated currents to NMDAR internalization. Indeed, direct application of glycine beyond the saturation threshold of glycine-B site primes NMDARs for endocytosis (Nong et al., 2003; Martina et al., 2005). Thus, moderate sub-threshold increases in extracellular glycine may be more effective in achieving an enhanced contribution of NMDAR-mediated currents to neuronal network functioning. Our data may be taken as support of this

view, because the elevation in extracellular glycine is expected to be higher and more widespread in EMX/GlyT1-KO than in CamKII/GlyT1-KO mice. However, there was no evidence that glycine-primed NMDAR internalization had led to a reduction in the abundance of NMDARs in EMX/GlyT1-KO mice, because these mice showed a normal expression level of the obligatory NR1 subunit of the NMDAR.

In addition, glycine also produces direct neuronal inhibition via activation of strychnine-sensitive glycine receptors (GlyAR). GlyARs are present in forebrain, although they are most abundant in the brain stem and spinal cord (Bechade et al., 1994; Rajendra et al., 1997). GlyT1 expressed in glia cells adjacent to GlyAR-containing inhibitory glycinergic neurons (Aragon and Lopez-Corcuera, 2005) contributes to the termination of inhibitory neurotransmission by removing glycine form the synaptic cleft (Gomeza et al., 2003). Because glia-associated GlyT1 is disrupted in EMX/GlyT1-KO but not in CamKII/GlyT1-KO mice, GlyAR-mediated neuronal inhibition is more likely to be enhanced in the former but not the latter mutant mice. This represents another mechanism whereby hippocampal network NMDAR-mediated currents were only substantially enhanced in CamKII/GlyT1-KO but not EMX/GlyT1-KO mice.

These possible regulatory mechanisms are not mutually exclusive, and they may collectively underlie the difference in NMDAR-mediated currents existing between these two mutant mouse lines, which clearly diverge in terms of several critical behavioral phenotypes related to different forms of memory processes as outlined below.

## EMX/GlyT1-KO does not enhance associative learning and reversal learning

Enhance aversive Pavlovian conditioning was a consistent and robust finding in CamKII/GlyT1-KO mice, which was further accompanied by the potentiation of the LI effect (Yee et al., 2006). An identical effect has also been observed with GlyT1 inhibiting drugs (Lipina et al., 2005; Black et al., 2009), which essentially is opposite to the effect of NMDAR antagonist on LI expression (Gaisler-Salomon and Weiner, 2003; Gaisler-Salomon et al., 2008). By contrast, there was no indication that such phenotypes were present in the EMX/GlyT1 mice – these null findings were equally robust and demonstrated across paradigms. Given that the paradigms selected including the behavioural parameters and apparatus are identical between the two studies, it is reasonable to address what might be the critical determinants for the presence or absence of these phenotypes in the two GlyT1 knockout lines. One possibility is may be whether hippocampal NMDAR-mediated currents were enhanced or not, because hippocampal NMDARs are known to assume an important role in associative learning including the selective property of associative learning as exemplified by LI (Gruart and Delgado-Garcia, 2007; Martinez et al., 2007; Sahun et al., 2007; Valenzuela-Harrington et al., 2007). One parsimonious hypothesis posits that the selective enhancement of NMDAR-mediated currents in CamKII/GlyT1-KO mice facilitates not only the formation of [CS→US] associative links but also [CS→nothing] association (Mohler et al., 2008), thus leading to the dual phenotypes of enhanced conditioning and LI potentiation.

NMDAR-mediated activation in the hippocampus critically modulates hippocampus-dependent learning and memory processes (Morris et al., 1990; Nakazawa et al., 2003; Bannerman et al., 2006). Damage to the hippocampus is known to result in persistent responding and preservation in goal-directed behavior indicative of impaired behavioral inhibition. Based on the observation of facilitated reversal learning observed in CamKII/GlyT1-KO mice (Yee et al., 2006), we hypothesize that NMDAR-dependent currents may be involved in the flexible expression of alternative (even incompatible) learned responses necessary for the maintenance of adaptive goal-directed behavior against changing environmental contingency. The absence of a change in NMDAR-mediated EPSC in EMX/GlyT1-KO mice and lack of an effect in reversal learning may be relevant to this speculation.

### Object recognition is facilitated by EMX/GlyT1-KO in a delay-dependent manner

On the other hand, object familiarity judgement was enhanced following EMX/GlyT1-KO here. This phenotype has previously been reported in CamKII/GlyT1-KO mice (Yee et al., 2006), and a similar effect on social recognition memory has been shown following GlyT1inhibitor treatment (Depoortere et al., 2005; Boulay et al., 2008; Karasawa et al., 2008). Notably, the enhancement in performance was similarly delay-dependent in the two conditional GlyT1 knockout mutant lines, which was associated with enhanced novelty detection instead of reduced forgetting – i.e., both mutations increase exploration of the novel objects without affecting familiar object exploration.

Does the emergence of this common phenotype undermine the pivotal role of hippocampal NMDAR in learning and memory? One possible interpretation is that rhinal cortices may be more closely linked to object recognition memory (Aggleton et al., 1997; Brown et al., 2001) than the hippocampus whose precise modulatory function in recognition memory remains ill defined (Bowles et al., 2007; Suchan et al., 2008). Functional alternations to extra-hippocampal NMDARs common to EMX/GlyT1-KO and CamKII/GlyT1-KO may be responsible for their shared promnesic effect in object familiarity judgment. The assessment of NMDAR function in the cortex would therefore be required to identify the critical neuronal mechanisms involved in this shared phenotype.

### EMX/GlyT1-KO enhances spatial working memory function

Working memory was mildly enhanced by EMX/GlyT1-KO as evidenced by the presence of a modest (and significant) improvement from trial 1 to 2 in the mutant mice under conditions that control mice were no longer able to demonstrate a clear learning from trial 1 to 2. When the presence of proactive interference was examined, the analysis also indicated a numerical suggestion that EMX/GlyT1-KO was marginally less susceptible to interference of previously learned platform location. This parallels the performance enhancing effect of the GlyT1 inhibitor SSR504734 on a continuous delayed alternation task that taxes the flexible use of working memory (Singer et al., 2009a). Against this background, the absence of a clear effect on working memory function when GlyT1 deletion was restricted to forebrain neurons (Yee et al., 2006) is somewhat intriguing, because hippocampal NMDAR-mediated ESPC was elevated in this mutant mouse line and hippocampus plays a notable role in the modulation of working memory function (Steele and Morris, 1999; Lee and Kesner, 2002; Nakazawa et al., 2003; Yoshihara and Ichitani, 2004; Bannerman et al., 2008). However, prefrontal dopaminergic neurotransmission is also known to influence working memory (Kolb, 1984; Jones, 2002) perhaps via glutamate-dopamine interaction (Verma and Moghaddam, 1996; Romanides et al., 1999; Goto and Grace, 2008; Kruse et al., 2009). The possibility that precognitive effect of SSR504734 reported by Singer et al. (2009) may stem from the drug's concomitant ability to increase the prefrontal extra-cellular dopamine levels cannot be excluded (Depoortere et al., 2005; Singer et al., 2009a).

However, there was no evidence for any concomitant change in dopaminergic neurotransmission in our EMX/GlyT1-KO mice. This is consistent with our previous study showing the neuron-specific CamKII/GlyT1-KO essentially did not affect the magnitude of the motor enhancing effect of amphetamine although the peak response was slightly delayed (Yee et al., 2006). The normal motor response to amphetamine contrasts sharply with the pronounced attenuation of response to the other psychostimulant drug PCP. This specificity is consistent with the expectation that the molecular deletion of GlyT1 primarily potentiated NMDAR function, although the possibility that GlyT1 disruption or inhibition may influence downstream interaction between glutamate and dopamine transmission should not be ignored (Grace, 1991, 2000). For example, GlyT1 inhibition appears uniquely able to potentiate limbic glutamate-mediated facilitation of dopamine release in the mesolimbic dopamine system

(Leonetti et al., 2006): and such concerted physiological changes in multiple brain regions may be, to varying degrees, responsible for the pro-cognitive effects seen following EMX/GlyT1-KO or pharmacological inhibition of GlyT1 (Singer et al., 2009b).

### Conclusion

Our data demonstrate that GlyT1 inhibition represents a feasible approach to modulate cognitive processes, and are further suggestive of a differential impact on learning via selective (neuronal *versus* global) GlyT1-targeted manipulations. However, contrasting the phenotypes reported across studies with different mutant lines must be made with caution due to lack of direct experimental comparison. This caveat is especially relevant for the contrast between the presence and absence of specific phenotypes between different mouse lines. Concordant effects are more readily interpretable without reference to the magnitude of the individual mutation's effects, and one parsimonious view is that such common phenotypes stem from the shared molecular disturbance. Divergences between the EMX/GlyT1-KO and neuron-specific CamKII/GlyT1-KO lines are suggestive, but do not in themselves constitute a direct demonstration, of a functional dissociation between neuron- and glia-associated GlyT1 in the regulation of higher cognitive behavior, which can be more directly examined with a forebrain glia-specific gene knockout system becomes available. The future development of cell-type as well as region specific GlyT1 inhibition therapies (e.g. by gene therapies using cell-type and regionally restricted expression of antisense RNA directed against GlyT1) may provide novel and highly selective avenues in the treatment of cognitive disorders. This may be an important consideration for the viability of GlyT1 blockers as clinical tools, as current drugs are incapable in differentiating between neuronal and glial transporters.

## Acknowledgments

The present study was supported by ETH Zurich, the National Centre for Competence in Research (NCCR): Neural Plasticity and Repair, funded by the Swiss National Science Foundation (SNF), the SNF grant 3100-066855, and NIH grant MH083973. We thank Peter Schmid for his technical assistance, Jeanne Michel and Pascal Guela for their services in animal husbandry, and Dr. Frank Bootz for his veterinary supervision and expertise.

## ABBREVIATIONS

**aCSF**
: artificial cerebrospinal fluid

**ALX 5407**
: (*R*)-*N*[3-(4_fluorophenyl)-3-(4_phenyl-phenoxy)propyl]-sarcosine

**AMPAR**
: alpha-amino-3-hydroxy-5-methyl-4-isoxazolepropionic acid receptor

**ANCVOA**
: analysis of covariance

**ANOVA**
: analysis of variance

**CamKIIα**
: $Ca^{2+}$/calmodulin kinase IIα (CaMKIIα)

**Cre-recombinase**
: tyrosine recombinase from bacteriophage P1

**CS**

conditioned stimulus

**EDTA**
ethylendiamin-tetraacetat)

**EMX1**
drosophila homeobox gene empty spiracles (Ems) mouse homolog

**EPSC**
excitatory postsynaptic currents

**GlyT1**
glycine transporter 1

**HEPES**
4-(2-hydroxyethyl)-1-piperazineethanesulfonic acid

**ITI**
inter trial interval

**LI**
latent inhibition

**NBQX**
2,3-dihydroxy-6-nitro-7-sulfamoyl-benzo[f]quinoxaline-2,3-dione

**NMDAR**
*N*-methyl-D-aspartic acid receptor

**nPE**
non-pre-exposed

**PCP**
phencyclidine

**PCR**
polymerase chain reaction

**PE**
pre-exposed

**PGK**
phosphoglycerate kinase

**RNA**
Ribonucleic acid

**SDS- PAGE**
sodium dodecylsulfate polyacrylamide gel electrophoresis

**SSR504734**
2-Chloro-N-S-phenyl 2S-piperidin-2-yl methyl]-3-trifluoromethyl benzamide, monohydrochloride

**TBST**
10 mM Tris-HCl, pH 7.5, 150 mM NaCl, 0.05% Tween-20

**Tris**
tris-(hydroxymethyl)-aminomethane

**Triton-X 100**

$C_{34}H_{62}O_{11}$

**Tween20**

polyoxyethylen(20)-sorbitan-monolaurat

**US**

unconditioned stimulus

## References


Aggleton JP, Keen S, Warburton EC, Bussey TJ. Extensive cytotoxic lesions involving both the rhinal cortices and area TE impair recognition but spare spatial alternation in the rat. Brain Res Bull 1997;43:279–287. [PubMed: 9227838]

Aragon C, Lopez-Corcuera B. Glycine transporters: crucial roles of pharmacological interest revealed by gene deletion. Trends Pharmacol Sci 2005;26:283–286. [PubMed: 15925702]

Atkinson BN, Bell SC, De Vivo M, Kowalski LR, Lechner SM, Ognyanov VI, Tham CS, Tsai C, Jia J, Ashton D, Klitenick MA. ALX 5407: a potent, selective inhibitor of the hGlyT1 glycine transporter. Mol Pharmacol 2001;60:1414–1420. [PubMed: 11723250]

Aura J, Riekkinen P Jr. Blockade of NMDA receptors located at the dorsomedial prefrontal cortex impairs spatial working memory in rats. Neuroreport 1999;10:243–248. [PubMed: 10203316]

Bannerman DM, Rawlins JN, Good MA. The drugs don't work-or do they? Pharmacological and transgenic studies of the contribution of NMDA and GluR-A-containing AMPA receptors to hippocampal-dependent memory. Psychopharmacol (Berl) 2006;188:552–566.

Bannerman DM, Niewoehner B, Lyon L, Romberg C, Schmitt WB, Taylor A, Sanderson DJ, Cottam J, Sprengel R, Seeburg PH, Kohr G, Rawlins JN. NMDA receptor subunit NR2A is required for rapidly acquired spatial working memory but not incremental spatial reference memory. J Neurosci 2008;28:3623–3630. [PubMed: 18385321]

Bartko SJ, Winters BD, Cowell RA, Saksida LM, Bussey TJ. Perirhinal cortex resolves feature ambiguity in configural object recognition and perceptual oddity tasks. Learn Mem 2007;14:821–832. [PubMed: 18086825]

Bechade C, Sur C, Triller A. The inhibitory neuronal glycine receptor. Bioessays 1994;16:735–744. [PubMed: 7980477]

Bergeron R, Meyer TM, Coyle JT, Greene RW. Modulation of N-methyl-D-aspartate receptor function by glycine transport. Proc Natl Acad Sci U S A 1998;95:15730–15734. [PubMed: 9861038]

Betz H, Gomeza J, Armsen W, Scholze P, Eulenburg V. Glycine transporters: essential regulators of synaptic transmission. Biochemical Society Transactions 2006;34:55–58. [PubMed: 16417482]

Black MD, Varty GB, Arad M, Barak S, De Levie A, Boulay D, Pichat P, Griebel G, Weiner I. Procognitive and antipsychotic efficacy of glycine transport 1 inhibitors (GlyT1) in acute and neurodevelopmental models of schizophrenia: latent inhibition studies in the rat. Psychopharmacol (Berl) 2009;202:385–396.

Boulay D, Pichat P, Dargazanli G, Estenne-Bouhtou G, Terranova JP, Rogacki N, Stemmelin J, Coste A, Lanneau C, Desvignes C, Cohen C, Alonso R, Vige X, Biton B, Steinberg R, Sevrin M, Oury-Donat F, George P, Bergis O, Griebel G, Avenet P, Scatton B. Characterization of SSR103800, a selective inhibitor of the glycine transporter-1 in models predictive of therapeutic activity in schizophrenia. Pharmacol Biochem Behav 2008;91:47–58. [PubMed: 18621075]

Bowles B, Crupi C, Mirsattari SM, Pigott SE, Parrent AG, Pruessner JC, Yonelinas AP, Kohler S. Impaired familiarity with preserved recollection after anterior temporal-lobe resection that spares the hippocampus. Proc Natl Acad Sci U S A 2007;104:16382–16387. [PubMed: 17905870]

Brown A, Carlyle I, Clark J, Hamilton W, Gibson S, McGarry G, McEachen S, Rae D, Thorn S, Walker G. Discovery and SAR of org 24598-a selective glycine uptake inhibitor. Bioorg Med Chem Lett 2001;11:2007–2009. [PubMed: 11454468]

Chen L, Muhlhauser M, Yang CR. Glycine tranporter-1 blockade potentiates NMDA-mediated responses in rat prefrontal cortical neurons in vitro and in vivo. J Neurophysiol 2003;89:691–703. [PubMed: 12574447]

Crawley JN. Unusual behavioral phenotypes of inbred mouse strains. Trends Neurosci 1996;19:181–182. [PubMed: 8723201]

Cubelos B, Gimenez C, Zafra F. Localization of the GLYT1 Glycine Transporter at Glutamatergic Synapses in the Rat Brain. Cereb Cortex 2005;15:448–459. [PubMed: 15749988]

Davachi L, Goldman-Rakic PS. Primate rhinal cortex participates in both visual recognition and working memory tasks: functional mapping with 2-DG. J Neurophysiol 2001;85:2590–2601. [PubMed: 11387403]

Depoortere R, Dargazanli G, Estenne-Bouhtou G, Coste A, Lanneau C, Desvignes C, Poncelet M, Heaulme M, Santucci V, Decobert M, Cudennec A, Voltz C, Boulay D, Terranova JP, Stemmelin J, Roger P, Marabout B, Sevrin M, Vige X, Biton B, Steinberg R, Francon D, Alonso R, Avenet P, Oury-Donat F, Perrault G, Griebel G, George P, Soubrie P, Scatton B. Neurochemical, electrophysiological and pharmacological profiles of the selective inhibitor of the glycine transporter-1 SSR504734, a potential new type of antipsychotic. Neuropsychopharmacol 2005;30:1963–1985.

Eulenburg V, Armsen W, Betz H, Gomeza J. Glycine transporters: essential regulators of neurotransmission. Trends Biochem Sci 2005;30:325–333. [PubMed: 15950877]

Feldon J, Weiner I. The latent inhibition model of schizophrenic attention disorder. Haloperidol and sulpiride enhance rats' ability to ignore irrelevant stimuli. Biol Psychiatry 1991;29:635–646. [PubMed: 2054435]

Gabernet L, Pauly-Evers M, Schwerdel C, Lentz M, Bluethmann H, Vogt K, Alberati D, Mohler H, Boison D. Enhancement of the NMDA receptor function by reduction of glycine transporter-1 expression. Neurosci Lett 2005;373:79–84. [PubMed: 15555781]

Gadea A, Lopez-Colome AM. Glial transporters for glutamate, glycine, and GABA III. Glycine transporters. J Neurosci Res 2001;64:218–222. [PubMed: 11319765]

Gaisler-Salomon I, Weiner I. Systemic administration of MK-801 produces an abnormally persistent latent inhibition which is reversed by clozapine but not haloperidol. Psychopharmacology (Berl) 2003;166:333–342. [PubMed: 12599023]

Gaisler-Salomon I, Diamant L, Rubin C, Weiner I. Abnormally persistent latent inhibition induced by MK801 is reversed by risperidone and by positive modulators of NMDA receptor function: differential efficacy depending on the stage of the task at which they are administered. Psychopharmacology (Berl) 2008;196:255–267. [PubMed: 17928997]

Gomeza J, Hulsmann S, Ohno K, Eulenburg V, Szoke K, Richter D, Betz H. Inactivation of the glycine transporter 1 gene discloses vital role of glial glycine uptake in glycinergic inhibition. Neuron 2003;40:785–796. [PubMed: 14622582]

Goto Y, Grace AA. Dopamine modulation of hippocampal-prefrontal cortical interaction drives memory-guided behavior. Cereb Cortex 2008;18:1407–1414. [PubMed: 17934187]

Grace AA. Phasic versus tonic dopamine release and the modulation of dopamine system responsivity: a hypothesis for the etiology of schizophrenia. Neuroscience 1991;41:1–24. [PubMed: 1676137]

Grace AA. The tonic/phasic model of dopamine system regulation and its implications for understanding alcohol and psychostimulant craving. Addiction 2000;95(Suppl 2):S119–128. [PubMed: 11002907]

Gruart A, Delgado-Garcia JM. Activity-dependent changes of the hippocampal CA3-CA1 synapse during the acquisition of associative learning in conscious mice. Genes Brain Behav 2007;6(Suppl 1):24–31. [PubMed: 17543036]

Harsing LG Jr, Gacsalyi I, Szabo G, Schmidt E, Sziray N, Sebban C, Tesolin-Decros B, Matyus P, Egyed A, Spedding M, Levay G. The glycine transporter-1 inhibitors NFPS and Org 24461: a pharmacological study. Pharmacol Biochem Behav 2003;74:811–825. [PubMed: 12667895]

Hashimoto K, Fujita Y, Ishima T, Chaki S, Iyo M. Phencyclidine-induced cognitive deficits in mice are improved by subsequent subchronic administration of the glycine transporter-1 inhibitor NFPS and D-serine. European Neuropsychopharmacology 2008;18:414–421. [PubMed: 17804206]

Hauser J, Rudolph U, Keist R, Mohler H, Feldon J, Yee BK. Hippocampal alpha5 subunit-containing GABAA receptors modulate the expression of prepulse inhibition. Mol Psychiatry 2005;10:201–207. [PubMed: 15263904]

Hodges H, Sowinski P, Sinden JD, Netto CA, Fletcher A. The selective 5-HT3 receptor antagonist, WAY100289, enhances spatial memory in rats with ibotenate lesions of the forebrain cholinergic projection system. Psychopharmacology (Berl) 1995;117:318–332. [PubMed: 7770608]

Iwasato T, Datwani A, Wolf AM, Nishiyama H, Taguchi Y, Tonegawa S, Knopfel T, Erzurumlu RS, Itohara S. Cortex-restricted disruption of NMDAR1 impairs neuronal patterns in the barrel cortex. Nature 2000;406:726–731. [PubMed: 10963597]

Javitt DC, Hashim A, Sershen H. Modulation of striatal dopamine release by glycine transport inhibitors. Neuropsychopharmacology 2005;30:649–656. [PubMed: 15688094]

Javitt DC, Sershen H, Hashim A, Lajtha A. Inhibition of striatal dopamine release by glycine and glycyldodecylamide. Brain Res Bull 2000;52:213–216. [PubMed: 10822163]

Jones MW. A comparative review of rodent prefrontal cortex and working memory. Curr Mol Med 2002;2:639–647. [PubMed: 12420803]

Karasawa JI, Hashimoto K, Chaki S. D-Serine and a glycine transporter inhibitor improve MK-801-induced cognitive deficits in a novel object recognition test in rats. Behavioural Brain Research 2008;186:78–83. [PubMed: 17854919]

Kawabe K, Ichitani Y, Iwasaki T. Effects of intrahippocampal AP5 treatment on radial-arm maze performance in rats. Brain Res 1998a;781:300–306. [PubMed: 9507170]

Kawabe K, Yoshihara T, Ichitani Y, Iwasaki T. Intrahippocampal D-cycloserine improves MK-801-induced memory deficits: radial-arm maze performance in rats. Brain Res 1998b;814:226–230. [PubMed: 9838131]

Kinney GG, Sur C, Burno M, Mallorga PJ, Williams JB, Figueroa DJ, Wittmann M, Lemaire W, Conn PJ. The glycine transporter type 1 inhibitor N-[3-(4′-fluorophenyl)-3-(4′-phenylphenoxy)propyl] sarcosine potentiates NMDA receptor-mediated responses in vivo and produces an antipsychotic profile in rodent behavior. J Neurosci 2003;23:7586–7591. [PubMed: 12930797]

Kolb B. Functions of the frontal cortex of the rat: a comparative review. Brain Res 1984;320:65–98. [PubMed: 6440660]

Kruse MS, Premont J, Krebs MO, Jay TM. Interaction of dopamine D1 with NMDA NR1 receptors in rat prefrontal cortex. Eur Neuropsychopharmacol 2009;19:296–304. [PubMed: 19186032]

Lee I, Kesner RP. Differential contribution of NMDA receptors in hippocampal subregions to spatial working memory. Nat Neurosci 2002;5:162–168. [PubMed: 11780144]

Leonetti M, Desvignes C, Bougault I, Souilhac J, Oury-Donat F, Steinberg R. 2-Chloro-N-[(S)-phenyl [(2S)-piperidin-2-yl] methyl]-3-trifluoromethyl benzamide, monohydrochloride, an inhibitor of the glycine transporter type 1, increases evoked-dopamine release in the rat nucleus accumbens in vivo via an enhanced glutamatergic neurotransmission. Neuroscience 2006;137:555–564. [PubMed: 16289893]

Lindsley CW, Wolkenberg SE, Kinney GG. Progress in the preparation and testing of glycine transporter type-1 (GlyT1) inhibitors. Current Topics in Medicinal Chemistry 2006;6:1883–1896. [PubMed: 17017963]

Lipina T, Labrie V, Weiner I, Roder J. Modulators of the glycine site on NMDA receptors, D-serine and ALX 5407, display similar beneficial effects to clozapine in mouse models of schizophrenia. Psychopharmacology (Berl) 2005;179:54–67. [PubMed: 15759151]

Lubow RE. Latent inhibition. Psychol Bull 1973;79:398–407. [PubMed: 4575029]

Lubow RE, Moore AU. Latent inhibition: the effect of nonreinforced pre-exposure to the conditional stimulus. J Comp Physiol Psychol 1959;52:415–419. [PubMed: 14418647]

Mackintosh, NJ. Stimulus selection: Learning to ignore stimuli that predict no change in reinforcement. In: RAHJS-H, editor. Constraints on learning. London: Academic Press; 1973. p. 75-96.

Martina M, ME BT, Halman S, Tsai G, Tiberi M, Coyle JT, Bergeron R. Reduced glycine transporter type 1 expression leads to major changes in glutamatergic neurotransmission of CA1 hippocampal neurones in mice. J Physiol 2005;563:777–793. [PubMed: 15661817]

Martinez LA, Klann E, Tejada-Simon MV. Translocation and activation of Rac in the hippocampus during associative contextual fear learning. Neurobiol Learn Mem 2007;88:104–113. [PubMed: 17363298]

McHugh TJ, Blum KI, Tsien JZ, Tonegawa S, Wilson MA. Impaired hippocampal representation of space in CA1-specific NMDAR1 knockout mice. Cell 1996;87:1339–1349. [PubMed: 8980239]

Meyer U, Chang DL, Feldon J, Yee BK. Expression of the CS- and US-pre-exposure effects in the conditioned taste aversion paradigm and their abolition following systemic amphetamine treatment in C57BL6/J mice. Neuropsychopharmacology 2004;29:2140–2148. [PubMed: 15238994]

Meyer U, Feldon J, Schedlowski M, Yee BK. Towards an immuno-precipitated neurodevelopmental animal model of schizophrenia. Neurosci Biobehav Rev 2005;29:913–947. [PubMed: 15964075]

Mohler H, Rudolph U, Boison D, Singer P, Feldon J, Yee BK. Regulation of cognition and symptoms of psychosis: Focus on GABA(A) receptors and glycine transporter 1. Pharmacology Biochemistry and Behavior 2008;90:58–64.

Morris RG, Davis S, Butcher SP. Hippocampal synaptic plasticity and NMDA receptors: a role in information storage? Philos Trans R Soc Lond B Biol Sci 1990;329:187–204. [PubMed: 1978364]

Nakazawa K, Sun LD, Quirk MC, Rondi-Reig L, Wilson MA, Tonegawa S. Hippocampal CA3 NMDA receptors are crucial for memory acquisition of one-time experience. Neuron 2003;38:305–315. [PubMed: 12718863]

Nong Y, Huang YQ, Ju W, Kalia LV, Ahmadian G, Wang YT, Salter MW. Glycine binding primes NMDA receptor internalization. Nature 2003;422:302–307. [PubMed: 12646920]

Pitsikas N, Boultadakis A, Sakellaridis N. Effects of sub-anesthetic doses of ketamine on rats' spatial and non-spatial recognition memory. Neuroscience 2008;154:454–460. [PubMed: 18472348]

Rajendra S, Lynch JW, Schofield PR. The glycine receptor. Pharmacol Ther 1997;73:121–146. [PubMed: 9131721]

Richmond MA, Murphy CA, Pouzet B, Schmid P, Rawlins JN, Feldon J. A computer controlled analysis of freezing behaviour. J Neurosci Methods 1998;86:91–99. [PubMed: 9894789]

Romanides AJ, Duffy P, Kalivas PW. Glutamatergic and dopaminergic afferents to the prefrontal cortex regulate spatial working memory in rats. Neuroscience 1999;92:97–106. [PubMed: 10392833]

Sahun I, Delgado-Garcia JM, Amador-Arjona A, Giralt A, Alberch J, Dierssen M, Gruart A. Dissociation between CA3-CA1 synaptic plasticity and associative learning in TgNTRK3 transgenic mice. J Neurosci 2007;27:2253–2260. [PubMed: 17329422]

Singer P, Feldon J, Yee BK. The glycine transporter 1 inhibitor SSR504734 enhances working memory performance in a continuous delayed alternation task in C57BL/6 mice. Psychopharmacology (Berl) 2009a;202:371–384. [PubMed: 18758757]

Singer P, Feldon J, Yee BK. Interactions between the glycine transporter 1(GlyT1) inhibitor SSR504734 and psychoactive drugs in mouse motor behaviour. Eur Neuropsychopharmacol. 2009b

Singer P, Boison D, Mohler H, Feldon J, Yee BK. Enhanced recognition memory following glycine transporter 1 deletion in forebrain neurons. Behav Neurosci 2007;121:815–825. [PubMed: 17907814]

Singer P, Yee BK, Boison D, Mohler H, Feldon J. Enhanced cognitive flexibility and adaptability following forebrain neuronal deletion of glycine transporter 1. Behavioural Pharmacology 2008;19:669–669.

Steele RJ, Morris RG. Delay-dependent impairment of a matching-to-place task with chronic and intrahippocampal infusion of the NMDA-antagonist D-AP5. Hippocampus 1999;9:118–136. [PubMed: 10226773]

Suchan B, Gayk AE, Schmid G, Koster O, Daum I. Hippocampal involvement in recollection but not familiarity across time: a prospective study. Hippocampus 2008;18:92–98. [PubMed: 17932973]

Sur C, Kinney GG. Glycine transporter 1 inhibitors and modulation of NMDA receptor-mediated excitatory neurotransmission. Current Drug Targets 2007;8:643–649. [PubMed: 17504107]

Tang Y-P, Shimizu E, Dube GR, Rampon C, Kerchner GA, Zhuo M, Liu G, Tsien JZ. Genetic enhancement of learning and memory in mice. Nature 1999;401:63–69. [PubMed: 10485705]

Tonegawa S, Nakazawa K, Wilson MA. Genetic neuroscience of mammalian learning and memory. Philos Trans R Soc Lond B Biol Sci 2003;358:787–795. [PubMed: 12740125]

Tsai G, Ralph-Williams RJ, Martina M, Bergeron R, Berger-Sweeney J, Dunham KS, Jiang Z, Caine SB, Coyle JT. Gene knockout of glycine transporter 1: characterization of the behavioral phenotype. Proc Natl Acad Sci U S A 2004;101:8485–8490. [PubMed: 15159536]

Tsien JT, Huerta PT, Tonegawa S. The essential role of hippocampal CA1 NMDA receptor-dependent synaptic plasticity in spatial memory. Cell 1996;87:1327–1338. [PubMed: 8980238]

Valenzuela-Harrington M, Gruart A, Delgado-Garcia JM. Contribution of NMDA receptor NR2B subunit to synaptic plasticity during associative learning in behaving rats. Eur J Neurosci 2007;25:830–836. [PubMed: 17328778]

Verma A, Moghaddam B. NMDA receptor antagonists impair prefrontal cortex function as assessed via spatial delayed alternation performance in rats: modulation by dopamine. J Neurosci 1996;16:373–379. [PubMed: 8613804]

Yee BK, Hauser J, Dolgov VV, Keist R, Mohler H, Rudolph U, Feldon J. GABA receptors containing the alpha5 subunit mediate the trace effect in aversive and appetitive conditioning and extinction of conditioned fear. Eur J Neurosci 2004;20:1928–1936. [PubMed: 15380015]

Yee BK, Balic E, Singer P, Schwerdel C, Grampp T, Gabernet L, Knuesel I, Benke D, Feldon J, Mohler H, Boison D. Disruption of glycine transporter 1 restricted to forebrain neurons is associated with a pro-cognitive and anti-psychotic phenotypic profile. J Neurosci 2006;26:3169–3181. [PubMed: 16554468]

Yoshihara T, Ichitani Y. Hippocampal N-methyl-D-aspartate receptor-mediated encoding and retrieval processes in spatial working memory: delay-interposed radial maze performance in rats. Neuroscience 2004;129:1–10. [PubMed: 15489023]

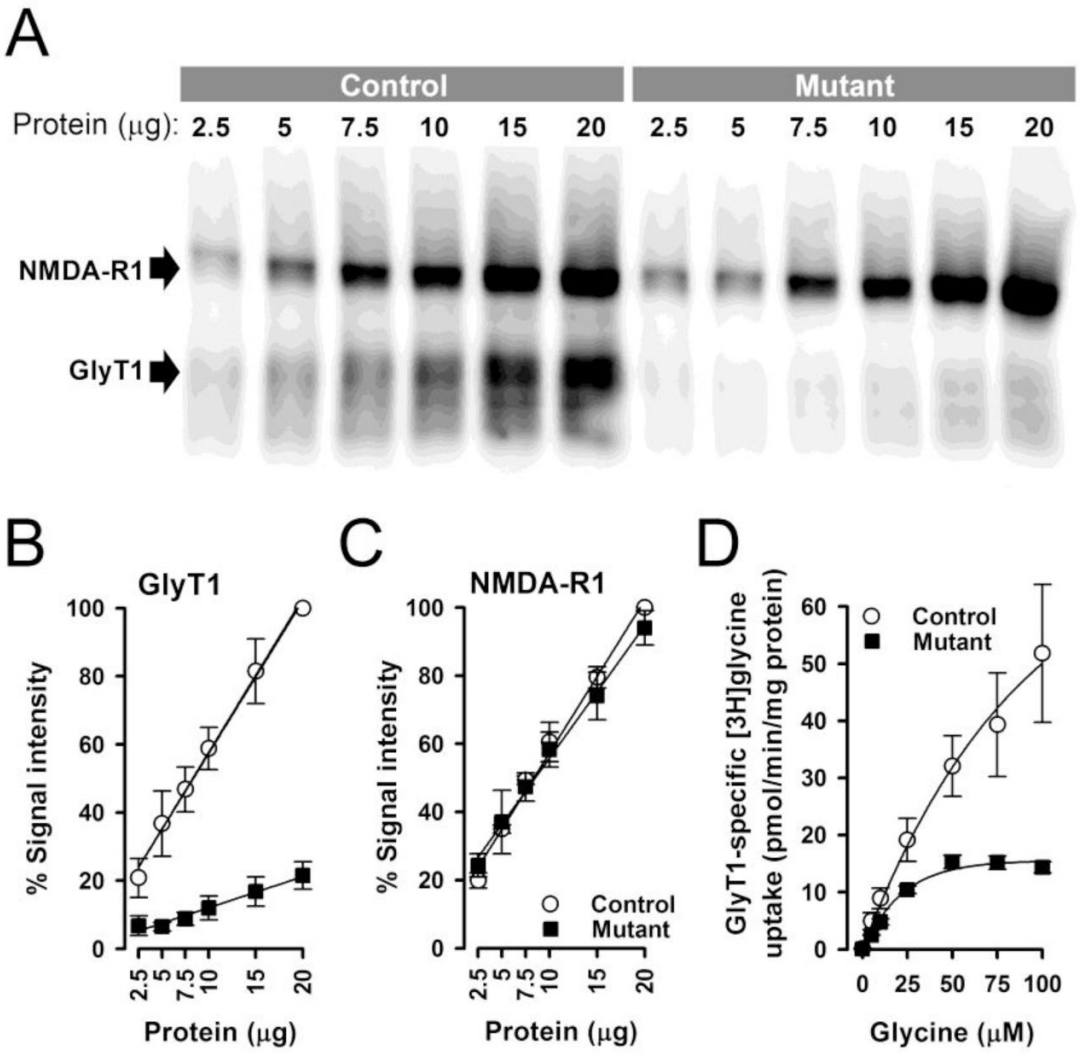


**Figure 1.**

GlyT1 and NMDA-N1 protein expression and [$^3$H]glycine uptake in the forebrain of mutant and control mice. GlyT1 and NMDA-R1 protein expressions levels in mutant and control mice were analyzed by Western blotting using increasing amounts of hippocampus/cortex membrane protein and GlyT1 as well as NMDA-R1 specific antibodies. A representative blot simultaneously probed for GlyT1 and NMDA-R1 immunoreactivity is depicted in ***A***. Expression of GlyT1, but NMDA-R1, was strongly reduced in the mutant mice. Quantification of the Western blots normalized to the GlyT1 (***B***) and NMDA-R1 (***C***) protein signal intensity at 20 micrograms in controls (100%). Data represent the mean +/− SD of four independent experiments. GlyT1-specific glycine transport into crude synaptosomal membranes prepared from hippocampus/cortex tissue of wild type and mutant mice was determined by measuring ALX5407-specific [$^3$H]-glycine uptake at increasing glycine concentrations (***D***). GlyT1-specific glycine uptake was markedly reduced in mutant mice. Data represent the mean ± standard error (SEM) of three independent experiments.

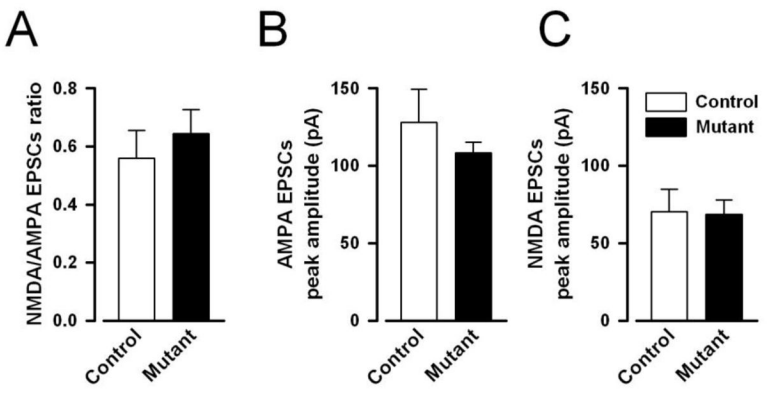


**Figure 2.**

NMDAR- and AMPAR-mediated EPSCs peak amplitude in CA1 pyramidal neurons of mutant and control mice. The ratio of NMDAR- to AMPAR-mediated EPSCs (A), AMPAR- (***B***) and NMDAR-mediated (***C***) currents did not differ between the two genotypes, indicating that the mutation did not affect the efficacy of AMPAR and NMDAR mediated neurotransmission in CA1 pyramidal neurons. All values refer to mean ± standard error of the mean (SEM).

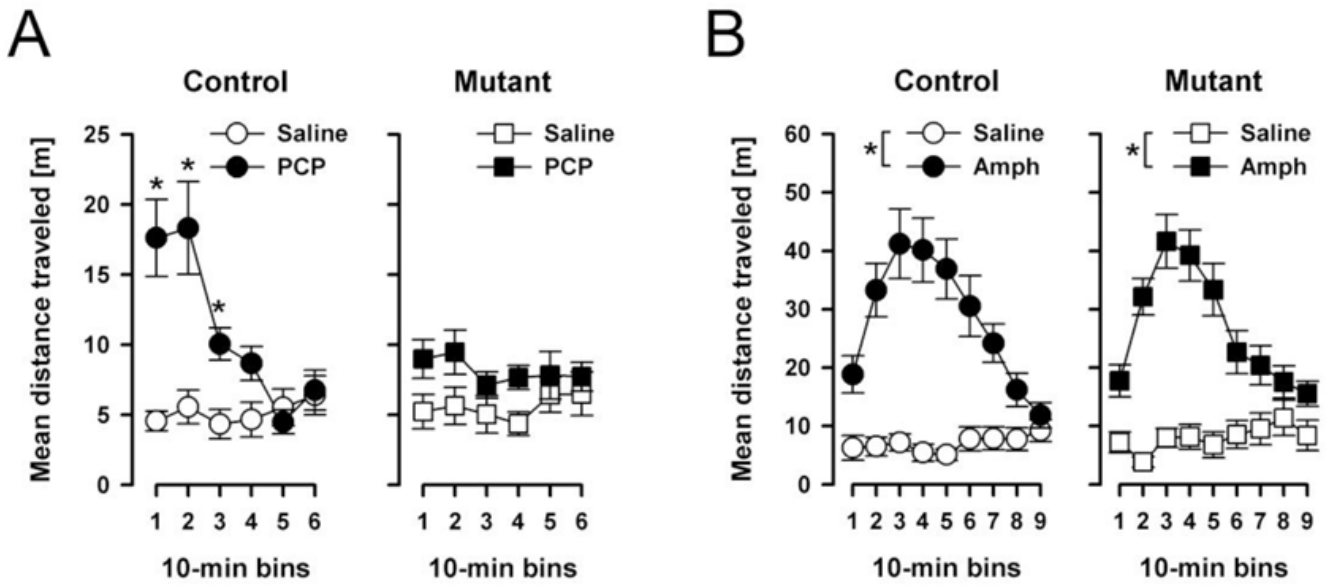


**Figure 3.**

The locomotor response to systemic PCP (A) and amphetamine (B). Locomotor activity was measured by distance moved of the animal's distance travelled in meter and summed into successive 10 min bins. (***A***) The motor stimulant effect of PCP was notably attenuated in mutants relative to controls in the first 30 min. Locomotor activity was comparable in mutants and controls after saline injection. The data analysis gave rise to a significant genotype × drug × bins interaction ($p<0.05$). (***B***) The mutation did not alter the motor stimulant effect of amphetamine. Similarly, mutants and controls did not differ in the saline condition. * Denotes that the distance travelled was significantly less ($p<0.05$) in the saline condition as compared to the PCP (***A***) and the amphetamine (***B***) condition, respectively All values refer to mean ± standard error of the mean (SEM).

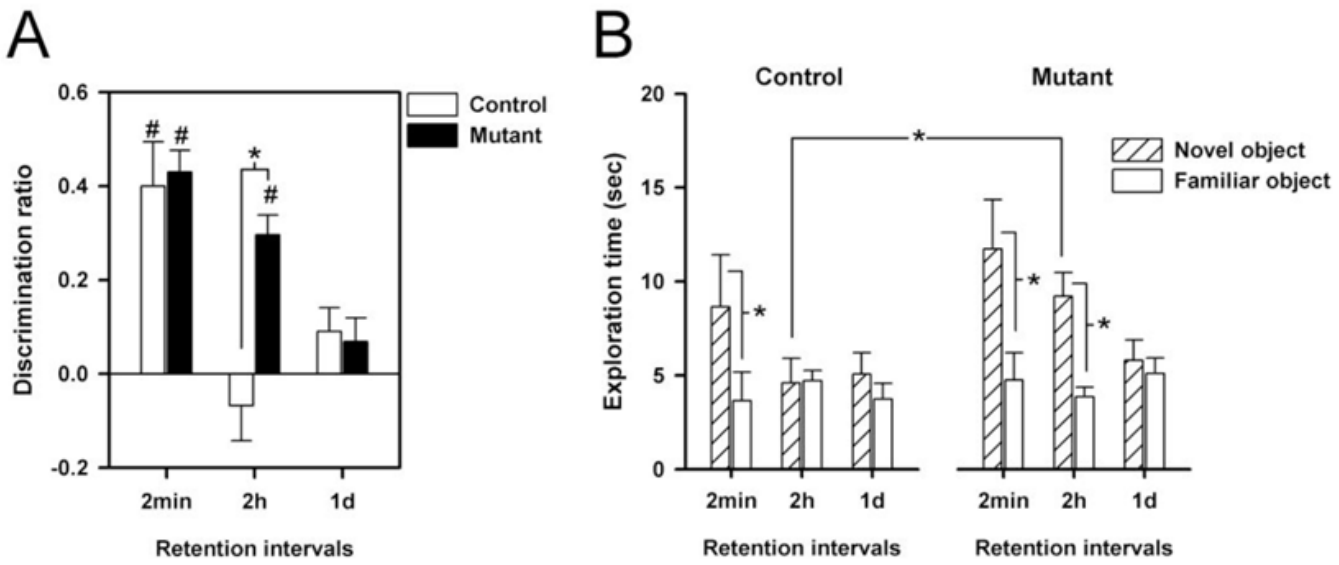


**Figure 4.**

Object recognition memory was indexed by the differential ratio defined as difference in exploration time towards the novel and the familiar objects divided by the total object exploration time with a positive ratio denoting a preference towards the novel objects (***A***). For comparison, the absolute exploration times towards the novel and the familiar objects are also illustrated (***B***). (***A***) Mutant mice showed an improved object recognition memory performance relative to controls at the 2h delay condition. This impression was confirmed by the occurrence of a significant main effect of genotype and of its interaction with delays (all p's<0.05) in a genotype × sex × delays ANOVA. Moreover, separated ANOVA's restricted to each delay revealed significant difference between mutant and controls on the 2h delay condition. * denotes a significant difference from control mice performance based on restricted analysis. # denotes that the differential ratio significantly differs from zero based on one-sample t-test. (***B***) Contrast between exploration times towards the novel vs. the familiar objects allows the evaluation of object recognition. Preference for the novel objects was apparent in the mutant and control mice at the shortest delay condition (* p<0.05). At 2-h delay, only mutant mice were able to maintain such a preference: this is associated with an enhanced exploration to the novel object in comparison to the controls (* p<0.05). All values refer to mean ± standard error of the mean (SEM).

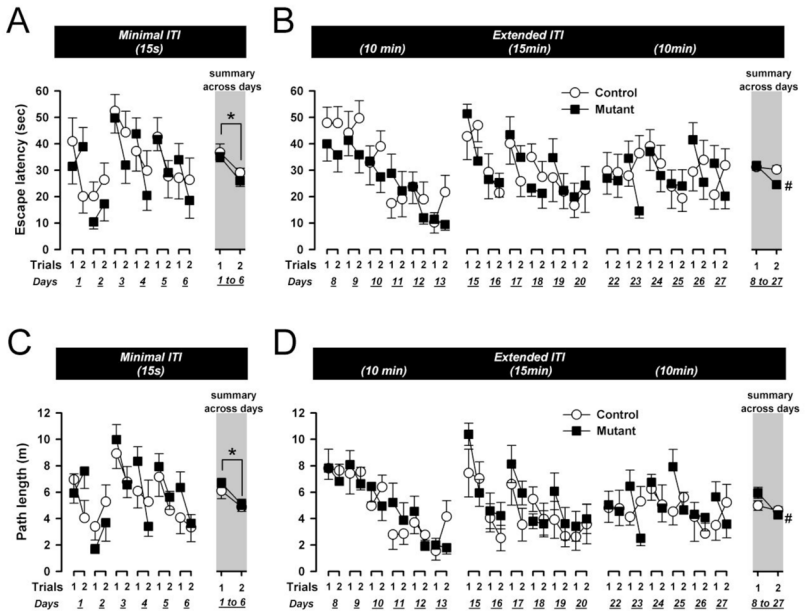


**Figure 5.**

Performance on the working memory task in the water maze as indexed by escape latency (***A*** & ***B***) and path length (***C*** & ***D***). Data are depicted across days and trials; and collapsed across days 1–6 (***A*** & ***C***) or across days 8–27 (***C*** & ***D***) in the summary portions (indicated by the gray background). At the minimal delay of 15sec, both groups of mice showed a comparable decrease in both the escape latency and the path length from trial 1 to trial 2 (collapsed across days) reflecting the presence of working memory in mutants and controls (*, $p<0.05$). Across the extended delay conditions (10–15min delays), working memory performance was somewhat improved in the mutants, as suggested by separate analyses indicating presence of a significant performance improvement in both measures from trial 1 to 2 in the mutants (#) but not controls. All values refer to mean ± standard error of the mean (SEM).

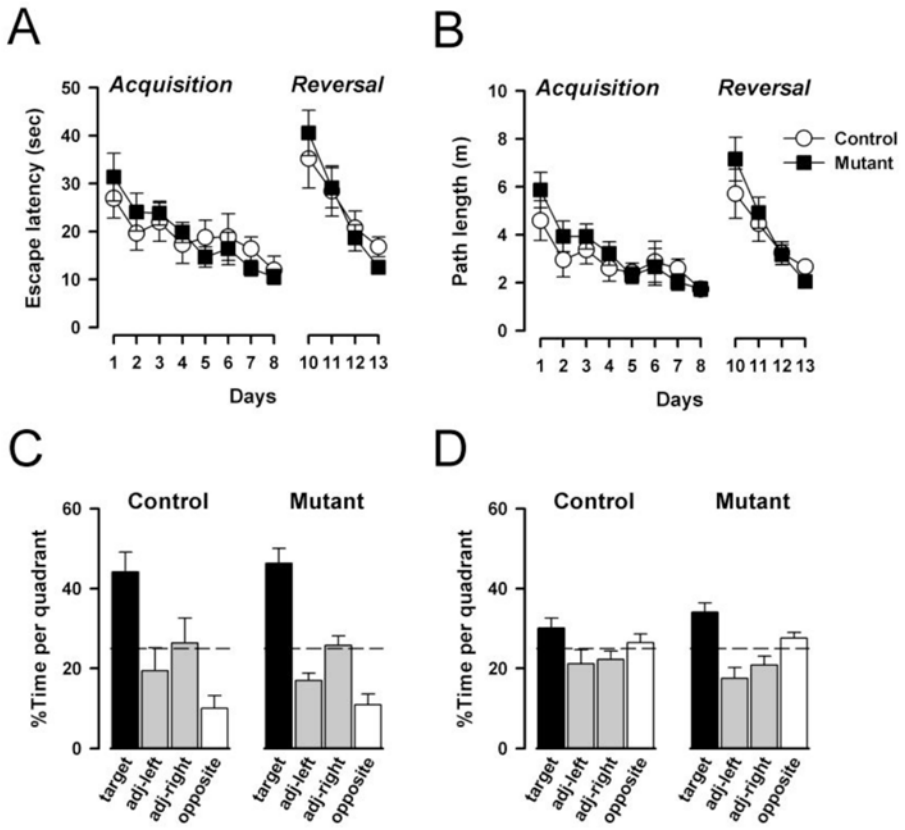


**Figure 6.**

Spatial reference memory and reversal learning. The mutation did not affect the reference memory learning in the initial acquisition session when the level of pro-active interference is expected to be minimal. This was equally seen in terms of escape latency (***A***) and path length (***B***). Similarly, mutants and control animals relearned the novel platform position at a similar rate in the second acquisition session when the animals were under the influence of proactive interference from the preceding reference memory session. Retention of reference memory was analyzed by the search preference for the trained quadrant in two probe tests, respectively. Probe test 1 (***C***) was conducted on day 8 prior to the acquisition training and probe test 2 (***D***) was conducted 24h after acquisition training on day 12. Both mutants and controls preferably searched in the trained quadrant in both probe tests suggesting that the mutation did not affect memory retention. The asterisk denotes that a significant difference from chance level according to Student's *t*-test ($p<0.05$). All values refer to mean ± standard error of the mean (SEM).

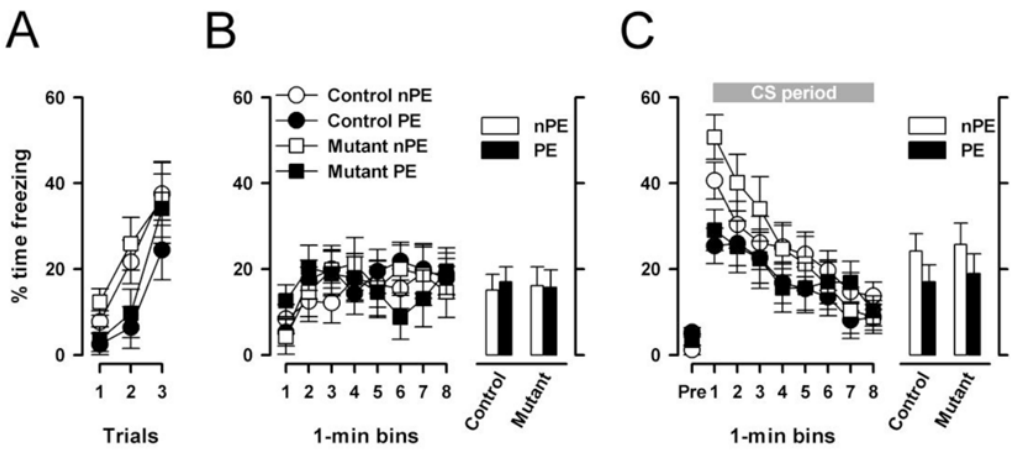


**Figure 7.**

LI in the conditioned freezing paradigm. (***A***), Expression of freezing behavior toward the tone-CS across the three conditioning trials immediately after pre-exposure. The amount of freezing was significantly reduced ($p<0.05$) in pre-exposed (PE) relative to non-pre-exposed (nPE) animals reflecting the LI effect. (***B***), Freezing to the context 24h after conditioning expressed as a function of 1 min bins on the left and as the overall means on the *right.* (***C***), Freezing to the tone CS 48h after conditioning. Freezing in the PE subjects tended to be lower than in the nPE subjects, which was more pronounced in the beginning of the CS-phase, which was equally seen in mutants and controls. This impression was confirmed by the appearance of a significant pre-exposure by bins interaction ($p<0.05$) in a 2 × 10 (pre-exposure × 1-min bins) ANOVA of the percent freezing. The histogram on the right illustrates the mean levels of freezing averaged across the entire 480s CS period. All values refer to mean ± standard error of the mean (SEM).

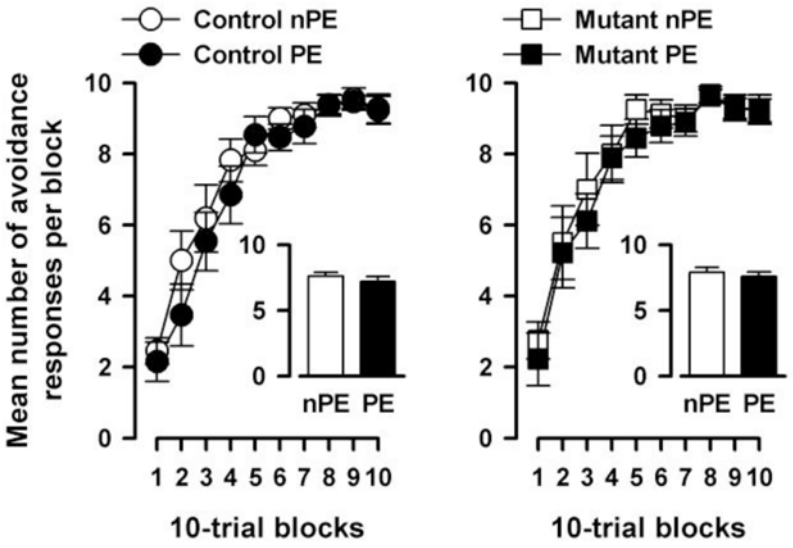


**Figure 8.**

LI in conditioned active avoidance learning. Acquisition of the conditioned avoidance response across 10 blocks of 10 trials conducted 24 h after tone pre-exposure in mutants (left) relative to controls (right). Learning was indexed by the percentage of avoidance trials. Increasing percent avoidance trials indicated the acquisition of avoidance learning as training progressed. The mean percentage of avoidance trials across the 10 blocks is illustrated in the histogram. PE and nPE refers to pre-exposed and non-pre-exposed animals, respectively. All values refer to mean ± standard error of the mean (SEM).

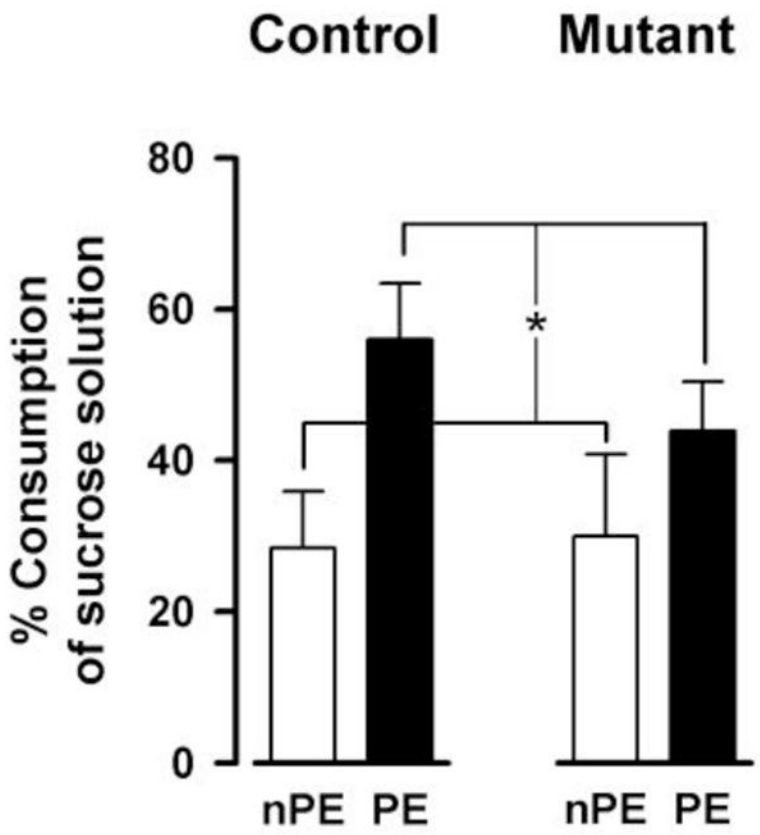


**Figure 9.**
LI in conditioned taste aversion. The expression of conditioned taste aversion on the test day (24h after sucrose-LiCl pairing) was indexed by the percentage of sucrose solution consumption in the 30 min test session. The lower the value the greater is the taste aversion. Weaker conditioned aversion in the pre-exposed (PE) relative to the non-pre-exposed (nPE) condition constitutes the LI effect (*$p < 0.05$). All values refer to mean ± standard error of the mean (SEM)..

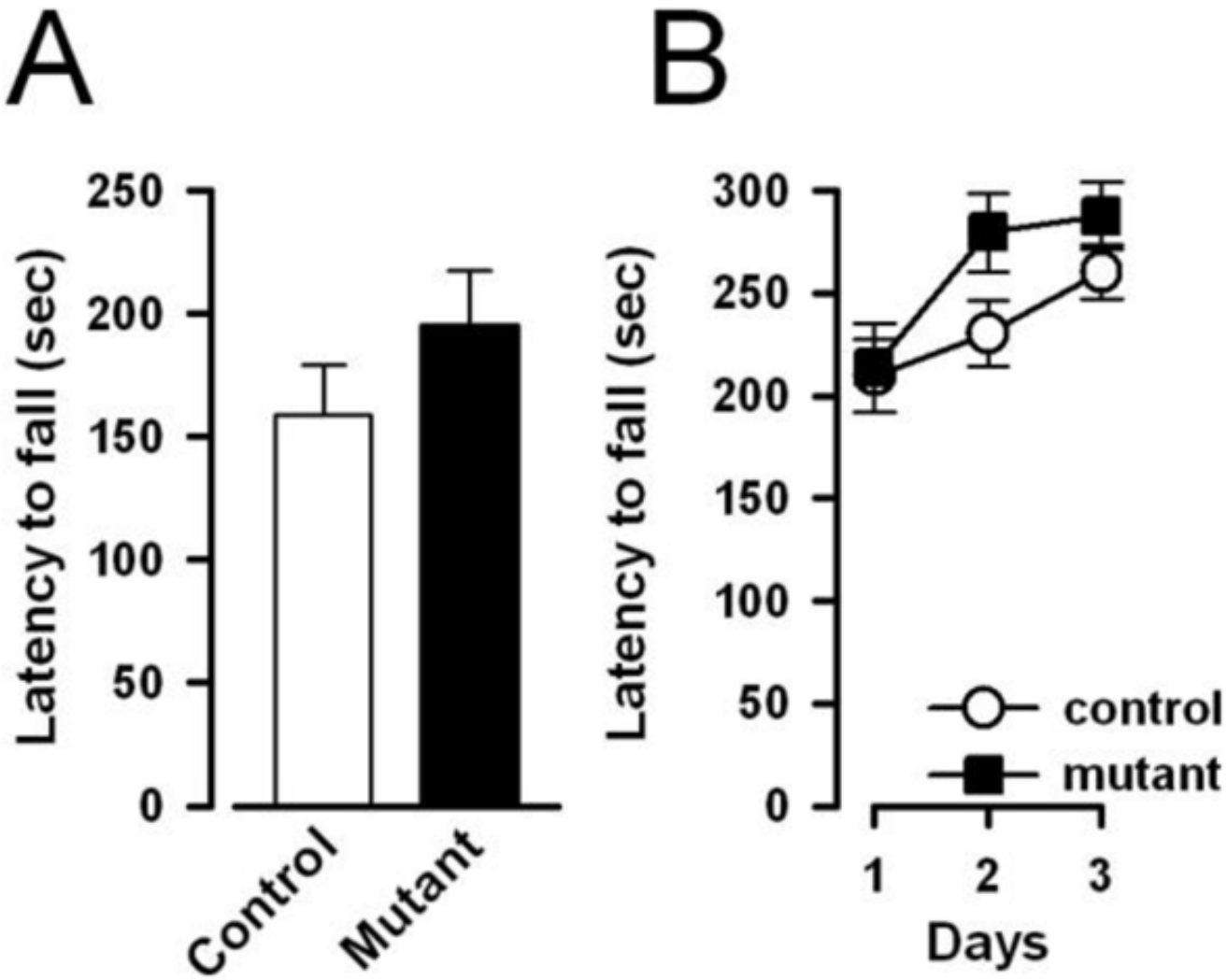


**Figure 10.**

Neuromuscular strength and motor coordination was as indexed by the latency to fall (in sec) from the hanging wire (***A***) and accelerating rotarod (***B***), respectively. The performance of mutant and controls animals appeared highly comparable across the two neurological tests indicating that the mutation did not affect motor functions. All values refer to mean ± standard error of the mean (SEM).

**Table 1**

Summary of test sequence, duration of each test, number of rest days between tests, and number of subjects accepted in the final analyses of each test.

| | | | | Control | | Mutant | |
|---|---|---|---|---|---|---|---|
| **Cohort** | **Sequence of Experiments** | **Duration** | **Post-test rest** | **♀** | **♂** | **♀** | **♂** |
| A | (1) Elevated plus maze | 1d | 2d | 11 | 13 | 10 | 7 |
| | (2) Hanging wire | 1d | 2d | 11 | 13 | 10 | 7 |
| | (3) Rotarod | 3d | 5d | 11 | 13 | 10 | 7 |
| | (4) Conditioned freezing | 3d | 10d | 6PE + 5nPE | 7PE + 6nPE | 5PE + 5nPE | 4PE + 3nPE |
| | (5) Active avoidance learning | 2d | 10d | 6PE + 5nPE | 6PE[a] + 6nPE | 5PE + 5nPE | 4PE + 3nPE |
| | (6) Response to PCP [b] | 1d | 10d | 5PCP + 5veh | 4PCP + 5veh | 5PCP + 5veh | 4PCP + 3veh |
| | (7) Response to amphetamine | 1d | | 5Amph + 5veh | 5Amph + 3veh | 5Amph + 5veh | 4Amph + 3veh |
| B | Conditioned taste aversion | 10d | | 7PE + 7nPE | 7PE + 7nPE | 5PE + 4nPE | 4PE + 5nPE |
| C | (1) Cued task in water maze | 1d | 0d | | 8 | | 10 |
| | (2) Working memory in water maze [c] | 27d | 7d | | 8 | | 10 |
| | (3) Reference memory in water maze | 13d | 13d | | 8 | | 10 |
| | (4) Object recognition memory | 14d | | 7 | 9 | 7 | 11 |

[a] Notes: one control mouse was dropped from the analysis due to failure of shock delivery during conditioning,

[b] only a maximum of 36 mice were possible to be tested together in a day,

[c] only male mice were included in the water maze test because of frequently observed floating behavior in female mice; one control and one mutant mice were further dropped from the final analysis due to excessive floating.

**Table 2**

Summary of liquid consumption on the days of pre-exposure, conditioning, and test phases of the conditioned taste aversion experiment. All values refer to mean ± standard error (SEM).

| | | Control | | Mutant | |
|---|---|---|---|---|---|
| **Experimental Phase** | **Consumption (in g)** | **nPE (n=14)** | **PE (n=14)** | **nPE (n=9)** | **PE nPE (n=9)** |
| Pre-exposure | Water | 1.35±0.09 | | 1.32±0.11 | |
| | Sucrose solution | | 1.79±0.10 | | 1.78±0.10 |
| Conditioning | Sucrose solution | 1.91±0.11 | 2.02±0.16 | 1.67±0.11 | 1.73±0.11 |
| Test | Sucrose solution | 0.26±0.07 | 0.64±0.10 | 0.36±0.16 | 0.53±0.10 |
| | Total liquid | 0.93±0.07 | 1.16±0.08 | 0.94±0.09 | 1.16±0.11 |